Anthracycline biosynthesis in Streptomyces: engineering, resistance and antimicrobial activity

Hulst, M.B.

Cryptic transporter genes that confer resistance to anthracyclines in *Streptomyces*

Mandy B. Hulst, Le Zhang, Chao Du, Hannah E. Augustijn, Thadee Grocholski, Dennis P.A. Wander, Mikko Metsä-Ketelä, Jacques J.C. Neefjes and Gilles P. van Wezel

Abstract

Doxorubicin (Doxo) is a potent anticancer drug produced by *Streptomyces peucetius*, but its clinical application is limited by severe dose-dependent side effects. *N*,*N*-dimethyldoxorubicin (DMdoxo) has emerged as a promising alternative, exhibiting comparable efficacy but with reduced side effects. However, biosynthesis of DMdoxo is challenging due to its intrinsic toxicity to the producer strain. Here we show that DMdoxo exerts higher antibacterial activity than Doxo itself, and that challenge with DMdoxo induces the activation of cryptic resistance export systems in streptomycetes unable to produce anthracyclines. Evolution of *Streptomyces lividans* TK24 for DMdoxo-resistant variants resulted in the emergence of spontaneous mutants. Transcriptome analysis of mutants with enhanced resistance revealed elevated expression of two gene pairs, *cdtAB* and *sclAB*, which both encode ATP-binding cassette transporters. Introduction of either transporter pair under the control of the constitutive *ermE** promoter conferred more than eight-fold increase in resistance in the parental strain to both Doxo and DMdoxo. Phylogenetic analysis of 629 genomes of Streptomycetaceae indicated that 12% of the genomes encode at least one transporter, suggesting a widespread resistance mechanism against anthracyclines. Thus, our study identified two cryptic transporters that are activated in response to anthracyclines, providing resistance to these compounds.

Introduction

Doxorubicin (Doxo), an anthracycline polyketide originally discovered in extracts of *Streptomyces peucetius* var. *caesius*, is a potent anticancer drug[11]. However, its clinical application is limited by significant side effects, including cardiotoxicity, therapy-related tumours, and infertility[13]. To address these limitations, extensive research efforts have been dedicated to the synthesis of Doxo derivatives through both biosynthesis and organic synthesis approaches. Among these alternative compounds, *N*,*N*-dimethyldoxorubicin (DMdoxo) has emerged as a promising candidate as it has lost most toxicities without loss in anticancer activities[16].

Anthracyclines are glycoside antibiotics with aglycones that are called anthracyclinones[30]. These compounds are categorised as aromatic type II polyketides, characterised by a linear tetracyclic structure with a 7,8,9,10-tetrahydro-5,12-naphthacenequinone scaffold, and are decorated with one or more sugar moieties. Anthracyclines exert their anticancer activities through DNA interaction, which results in two distinct effects: DNA damage, via the trapping and poisoning of topoisomerase II onto the DNA resulting in DNA double-strand breaks, and chromatin damage, involving the eviction of histones at defined sites in the genome[14,15]. Anthracyclines inducing both DNA double-strand breaks and histone eviction have been associated with cardiotoxicity, a major side effect of anthracycline drugs. In contrast, histone eviction activity alone is associated with limited side effects. *N*,*N*-dimethylation of Doxo resulted in the loss of DNA damage activity, while maintaining histone eviction activity with no loss in cytotoxicity[16]. Given that toxicity currently limits the treatment of cancer patients, this positions DMdoxo as a promising candidate for an improved anticancer drug that may even be used in a more chronic manner in cancer treatment.

Despite their efficacy as anticancer compounds, the DNA intercalating activity of anthracyclines evokes self-toxicity in the producer strain. Consequently, anthracycline-producing *Streptomyces* strains have evolved self-resistance mechanisms[266]. These mechanisms are encoded within the anthracycline biosynthetic gene clusters (BGCs) and play a crucial role in protecting the producer strains. Various self-resistance mechanisms against anticancer compounds encompass efflux, sequestration, modification, self-sacrifice, and metabolic dormancy[57]. Anthracycline BGCs typically harbour genes encoding ATP-binding cassette (ABC) transporters that facilitate the efflux of the produced compounds[266]. The daunorubicin BGC of *S. peucetius* comprises four genes involved in self-resistance. Among these, *drrA* and *drrB* encode an ABC transporter facilitating the efflux of daunorubicin and Doxo[64]. DrrC is homologous to UvrA-like proteins and is involved in recognising and repairing DNA damage[68]. The fourth gene, *drrD*, has also been implicated in resistance, although the exact mechanism remains unknown[66].

In principle, the biosynthesis of DMdoxo can be achieved by combining enzymes from the biosynthetic pathways of Doxo, aclacinomycin, and rhodomycin. However, despite the expression of all the necessary enzymes in an engineered *S. peucetius* strain, the crude extracts did not yield detectable levels of DMdoxo[293]. A key bottleneck may be the significant toxicity of

DMdoxo to the engineered strain, as it was 16-fold more toxic compared to Doxo. This finding suggests that it is imperative to develop a DMdoxo-resistant host to achieve biosynthesis of DMdoxo and evoked our interest in exploring anthracycline resistance mechanisms of actinomycetes. Actinomycetes are typically found in complex environments with diverse microbial communities, where they must protect their habitat from competitors[21,51]. They employ secondary metabolites for both communication and defence. Anthracyclines may also play a role in this complex ecological system. Consequently, it is plausible that other actinomycetes have evolved resistance mechanisms to mitigate the toxic effects of anthracyclines.

The primary goal of this study was to explore and uncover anthracycline resistance mechanisms in actinomycetes. We observed a relatively high frequency of Doxo resistance within our laboratory's actinomycete collection, while resistance to DMdoxo was far less common. The toxicity of DMdoxo explains why it is difficult or impossible to identify streptomycetes naturally producing this compound. Subsequently, we demonstrated that anthracycline resistance can be activated in strains that do not produce anthracyclines through adaptive laboratory evolution with DMdoxo. Through reverse engineering, we identified two cryptic transporters that confer resistance to both Doxo and DMdoxo. Finally, phylogenetic analysis revealed that the presence of homologs of the two transporters is relatively common and not correlated to the presence of anthracycline BGCs.

Results

Antimicrobial activity of doxorubicin and *N,N*-dimethyldoxorubicin

The anthracycline *N,N*-dimethyldoxorubicin (DMdoxo) is a promising effective anticancer compound with reduced side effects compared to doxorubicin (Doxo). However, biosynthesis efforts for DMdoxo face challenges due to the inherent sensitivity of *S. peucetius* to DMdoxo[293]. These results prompted us to explore anthracycline resistance mechanisms of actinomycetes. To assess the tolerance of *Streptomyces* species to Doxo and DMdoxo, we tested a panel of six strains, each known to produce different classes of aromatic polyketides. The panel consisted of *S. peucetius*, *Streptomyces galilaeus*, *Streptomyces venezuelae*, *Streptomyces rimosus*, *Streptomyces coelicolor* M145 and *Streptomyces lividans* TK24. *S. galilaeus* produces aclacinomycins, which are anthracyclines that are closely related to Doxo. *S. venezuelae* produces jadomycins, which belong to the angucyclines. Angucyclines are polyketides with a non-linear tetracyclic aglycone. *S. rimosus* produces the polyketide tetracycline. Furthermore, the panel included the model strains *S. coelicolor* M145 and *S. lividans* TK24 that are derivatives of the model strains *S. coelicolor* A3(2) and *S. lividans* 1326, which lack their genomic plasmids.

Each strain was spotted at a concentration of $1.0 \cdot 10^4$ CFU per spot onto SFM agar plates with increasing Doxo or DMdoxo concentrations. *S. venezuelae* and *S. rimosus* demonstrated surprisingly high resistance levels to Doxo and were able to grow in the presence of 256 µM or 512 µM Doxo, respectively (Figure 1). This finding is particularly striking when considering that

64 µM Doxo severely inhibited the growth of the model Doxo producer *S. peucetius*. Additionally, *S. coelicolor* M145 and *S. lividans* TK24 also demonstrated relatively high resistance, with growth at 32 µM or 64 µM Doxo, respectively. Interestingly, all of the strains were much more sensitive to DMdoxo than to Doxo, failing to grow at concentrations higher than 2 µM or 4 µM DMdoxo (Figure 1).

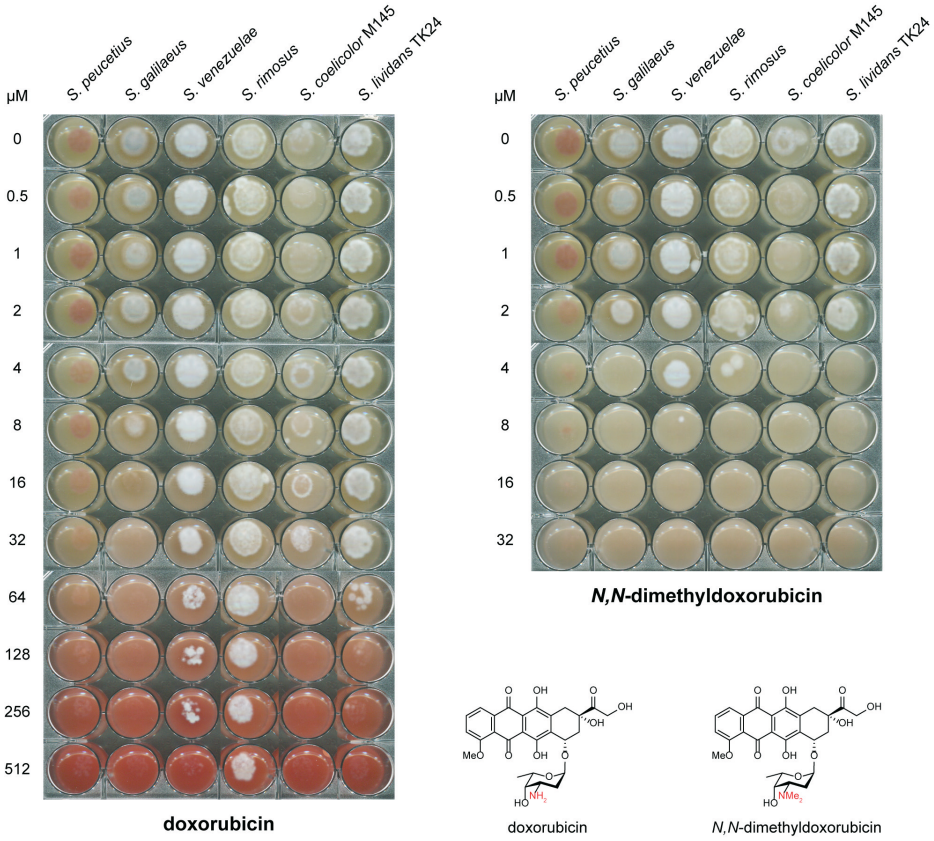

Figure 1. Sensitivity of selected *Streptomyces* strains against Doxo and DMdoxo. Anthracycline producers *S. peucetius* (produces Doxo) and *S. galilaeus* (produces aclarubicin), angucycline producer *S. venezuelae* (produces jadomycin), tetracycline producer *S. rimosus* and the model strains *S. coelicolor* M145 and *S. lividans* TK24 were spotted on SFM agar plates with 0.5 to 512 µM Doxo or 0.5 to 32 µM DMdoxo (both compounds are visible as red pigments). For each strain, 5 µL was spotted at a concentration of $1.0 \cdot 10^4$ CFU per spot and the plates were incubated at 30 °C for 4 days. All tested strains exhibited higher resistance to Doxo than to its close derivative DMdoxo.

To comprehensively evaluate resistance to Doxo and DMdoxo, we screened our in-house MBT collection, consisting of actinomycetes isolated from soil originating from the Himalaya mountain range in Nepal and the Qinling Mountains in China[294], Dutch dune soil, isolates from a wastewater treatment plant[295] and sponge-associated isolates[296]. Approximately 350 strains were spotted at high density onto SFM agar plates with 50 $\mu g \cdot mL^{-1}$ (i.e. 92 µM) Doxo

or 25 μg·mL^{-1} (i.e. 44 μM) DMdoxo. The strains exhibited large variation in their growth when exposed to the two compounds. About 40% of the strains demonstrated resistance to 50 μg·mL^{-1} (i.e. 92 μM) Doxo. About 31% of the strains demonstrated inhibited growth, while about 9% of the strains grew well and developed aerial hyphae or spores. In contrast, only six strains demonstrated growth in the presence of 25 μg·mL^{-1} (i.e. 44 μM) DMdoxo.

To illustrate the difference in toxicity of Doxo and DMdoxo, a subset of 72 representative strains is shown in Figure 2A. Each strain was spotted at high density onto SFM agar plates supplemented with 25 μM Doxo or DMdoxo. This revealed striking differences between colonies grown on Doxo or DMdoxo, showing that resistance to Doxo is relatively common, while resistance to DMdoxo is a rare phenomenon among actinomycetes. For example, when grown on Doxo, strains HP5 ("1" in Figure 2A), HP40 ("2") and Hm84 ("3") showed inhibition of development, slightly reduced growth, and normal growth, respectively, while the strains could not or hardly grow on DMdoxo. Six strains were selected that demonstrated growth at the high concentration of 25 μg·mL^{-1} (i.e. 44 μM) DMdoxo and studied in more detail. These strains were spotted at high density on SFM agar plates with increasing Doxo or DMdoxo concentrations. All strains demonstrated resistance to 200 μM Doxo, with a phenotype comparable to the control plate without Doxo (Figure 2B). Among these, *Streptomyces* sp. Els4, *Streptomyces* sp. Hm84 and *Streptomyces* sp. MBT74 demonstrated the highest resistance to DMdoxo and were able to grow in the presence of 200, 100 and 80 μM DMdoxo, respectively. However, growth and development were significantly inhibited by DMdoxo at the given concentrations, evident from the absence of aerial hyphae and spore formation. Els4, Hm84 and MBT74 showed normal growth and development at DMdoxo concentrations up to 80, 20 and 40 μM, respectively (Figure 2B).

Considering their high tolerance to Doxo and DMdoxo, the genomes of Els4, Hm84 and MBT74 were analysed in more detail. The whole genome sequences of Els4 and Hm84 were determined using Illumina sequencing, while the genome sequence of MBT74 was already available[294]. Draft genomes were assembled for Els4 and Hm84 resulting in 164 and 163 contigs, respectively (Supplementary Table S5). The genomes were analysed for the presence of putative biosynthetic gene clusters (BGCs) using antiSMASH 7.0[297], which were annotated using the MiBIG database[298]. We were particularly interested in the presence of anthracycline BGCs or other polyketide type II BGCs that may harbour resistance genes. Analysis of the Els4 genome predicted the presence of 38 putative BGCs (Supplementary Table S6), of which BGC2 showed very high similarity to the BGC for the angucycline warkmycin (MIBiG cluster BGC0001438, 97% similarity[299]). AntiSMASH predicted 21 putative BGCs in the genome of MBT74 (Supplementary Table S7), but no BGCs were detected for type II polyketides other than the BGC for the biosynthesis of a spore pigment. The Hm84 genome contained 37 putative BGCs (Supplementary Table S8), of which BGC37 showed high similarity with the BGC for the angucycline jadomycin (MIBiG cluster BGC000234, 85% similarity).

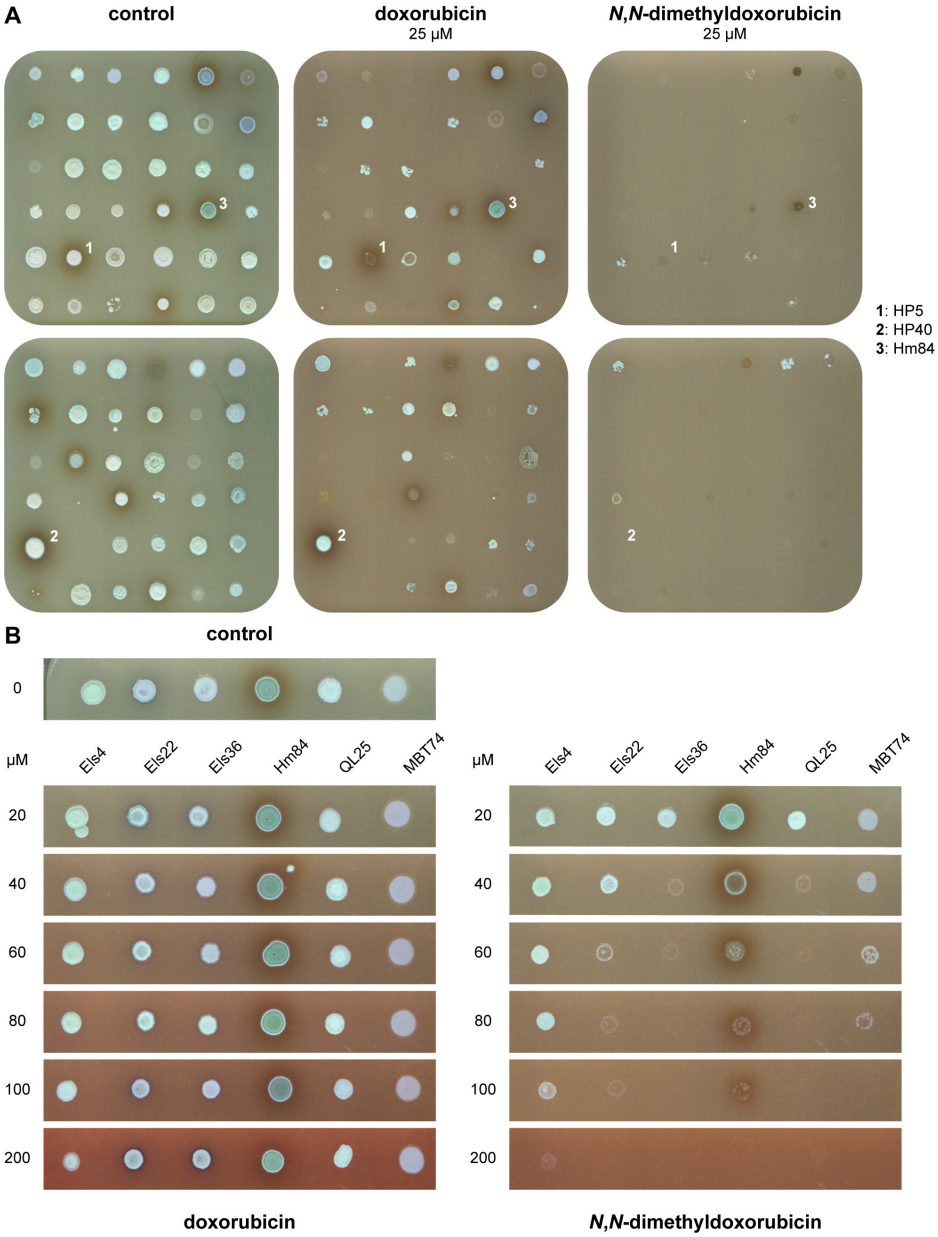

Figure 2. Resistance of wild-type actinomycetes against Doxo and DMdoxo. (A) A subset of 72 representative strains of our in-house collection of actinomycetes was spotted on SFM agar plates with 25 µM Doxo or DMdoxo. For each strain, 2 µL of highly concentrated spore or mycelial stock was spotted, and the plates were incubated at 30 °C for 3 days. Resistance to Doxo is more commonly observed than resistance to DMdoxo. *Streptomyces* sp. HP5, *Streptomyces* sp. HP40 and *Streptomyces* sp. Hm84 are indicated by 1, 2 and 3, respectively. **(B)** Six strains that displayed strong resistance to DMdoxo were spotted on SFM agar plates with 20 to 200 µM Doxo or DMdoxo. For each strain, 2 µL of highly concentrated or mycelial stock was spotted, and the plates were incubated at 30 °C for 3 days.

Both *S. venezuelae* and Hm84 harbour a jadomycin BGC and demonstrated relatively high resistance to Doxo. To test whether the presence of the jadomycin BGC may confer resistance to DMdoxo, the entire BGC was deleted from the genome of *S. venezuelae* as described[271]. The method makes use of the unstable multicopy vector pWHM3-oriT[280], which is a derivative of pWHM3[269] that harbours *oriT* to allow for its conjugative transfer. Approximately 1.5 kb regions flanking the jadomycin BGC (upstream of *jadR3* and downstream of *jadR**)[300] were amplified from genomic DNA using PCR, and the apramycin resistance gene *aacC4* was then cloned in between. The resulting knock-out construct (pGWS1447) was introduced into *S. venezuelae* via conjugation, and mutants were obtained by selecting for apramycin resistance and loss of thiostrepton resistance used for vector selection. Thus, we obtained a mutant where the entire BGC of jadomycin was replaced by the apramycin cassette, which is designated MAG409. Wild-type *S. venezuelae* and its mutant derivative MAG409 were spotted on SFM agar plates with increasing Doxo concentrations. Deletion of the jadomycin BGC did not affect the resistance of *S. venezuelae* to Doxo (Supplementary Figure S2).

Adaptive laboratory evolution generates anthracycline-resistant mutants

To activate cryptic anthracycline resistance mechanisms, we employed an adaptive laboratory evolution approach with a panel of streptomycetes. We hypothesised that anthracycline resistance mechanisms may be inactive under standard conditions and may be activated under evolutionary pressure. For this experiment, the panel of strains was comprised of *S. peucetius*, *S. galilaeus*, *S. coelicolor* A3(2), *S. lividans* TK24, *Streptomyces showdoensis* and *Streptomyces curacoi*. As discussed above, *S. peucetius* is a producer of Doxo, *S. galilaeus* is a producer of aclarubicin, *S. coelicolor* A3(2) is a wild-type model strain and *S. lividans* TK24 is a variant of wild-type strain *S. lividans* 1326 without genomic plasmids. *S. curacoi* and *S. showdoensis* were included to ensure a diverse panel of strains.

Evolution was achieved through serial propagation of batch cultures in TSB medium with progressively increasing DMdoxo concentrations (Figure 3A). In between transfers, strains were selected based on improved resistance as monitored by growth on SFM agar plates supplemented with different DMdoxo concentrations. The experiments were concluded once the strains demonstrated growth in TSB medium supplemented with 100 $\mu g \cdot mL^{-1}$ (i.e. 175 µM) DMdoxo, typically accomplished within ten transfers. Spore or mycelial stocks were prepared, and the evolved strains were labelled by adding "-Evo". To study the phenotypes of the parental and evolved strains and their levels of resistance, they were grown on SFM agar. Evolved isolates of both *S. coelicolor* and *S. galilaeus* displayed obvious developmental defects, manifested as a so-called "bald" (non-sporulating) phenotype, characterised by the absence of white aerial hyphae or grey spores (Figure 3B). In terms of their resistance, the parental strains were susceptible to 20 µM DMdoxo, except for *S. curacoi*, which could grow up to 40 µM DMdoxo (Supplementary Figure S3). *S. curacoi* also exhibited high levels of resistance to Doxo and could grow even in the presence of 200 µM Doxo. Among the evolved strains, TK24-EvoA1, *S. coelicolor*-Evo and *S. showdoensis*-Evo exhibited high levels of resistance, being able to grow in the presence of 200 µM Doxo or DMdoxo (Figure 3C). We decided to continue with TK24-EvoA1

for further investigation. *S. showdoensis*-Evo and *S. coelicolor*-Evo were excluded from further analysis, for reasons of lack of genetic tractability and lack of development, respectively.

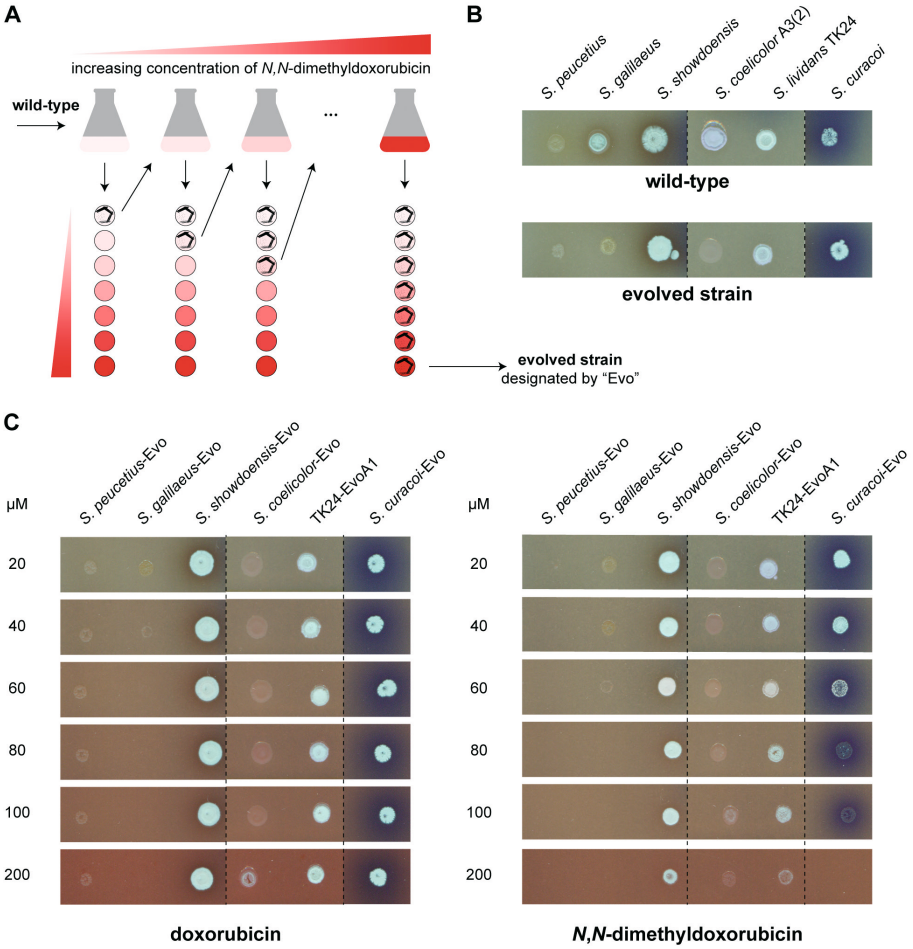

Figure 3. Adaptive laboratory evolution to obtain DMdoxo-resistant derivatives induces anthracycline resistance in various *Streptomyces* species. (A) Schematic representation of the adaptive laboratory evolution experiment with increasing DMdoxo concentrations. Wild-type strains were inoculated in TSB medium with sub-inhibitory levels of DMdoxo. Once the cultures reached stationary growth, they were streaked onto SFM agar plates with increasing DMdoxo concentrations. Biomass from the highest concentration that supported growth was then used to inoculate fresh TSB medium with the corresponding DMdoxo concentration. This process was repeated until a concentration of 100 μg·mL^{-1} (i.e. 175 μM) DMdoxo was achieved. **(B)** The parental and evolved strains of *S. peucetius*, *S. galilaeus*, *S. showdoensis*, *S. coelicolor* A3(2), *S. lividans* TK24 and *S. curacoi* were spotted on SFM agar plates. For each strain, 2 μL of highly concentrated spore or mycelial stock was spotted, and the plates were incubated at 30 °C for 3 days. Evolved isolates of *S. galilaeus* and *S. coelicolor* exhibited a 'bald' phenotype. **(C)** The parental and evolved strains were spotted on SFM agar plates with 20 to 200 μM Doxo or DMdoxo concentrations. For each strain, 2 μL of highly concentrated spore or mycelial stock was spotted, and the plates were incubated at 30 °C for 3 days. Evolved isolates of *S. showdoensis*, *S. coelicolor* and *S. lividans* TK24 exhibited the highest level of resistance to DMdoxo.

Whole-genome sequencing followed by Illumina paired-end sequencing was performed on TK24-EvoA1 to identify genomic variants that emerged during the evolution of TK24 (genome accession of the parental strain is NZ_CP009124.1). Genomic variant detection was performed using *breseq* v.0.38.1[301]. Mutations in pseudogene regions and silent mutations in coding regions were disregarded. Following these filtering steps, only three mutations were identified in TK24-EvoA1 (Table 1).

Table 1. Genomic variants identified in TK24 isolates from evolution experiments with DMdoxo.

Position*	Locus tag*	Variants	Annotation	Description	Isolate+
Genomic variants detected in evolution line A					
4,570,869	SLIV_RS 20695	substitution G→A	R71Q CGG→CAG	putative PadR-family transcriptional regulator (*cdtR*)	A1
4,571,366	SLIV_RS 20700	substitution C→A	intergenic 27	daunorubicin resistance protein DrrA-family ABC transporter ATPbinding subunit (*cdtA*)	A1
5,118,539	SLIV_RS 22890	insertion $C_{5\to6}$	frameshift 453/1482 nt	putative polysaccharide synthase (*matA*)	A1
Genomic variants detected in evolution line B					
1,743,319	SLIV_RS 07645	substitution G→A	P350S CCG→TCG	putative secreted hydrolase	B2–4
3,728,105	SLIV_RS 16660	substitution C→T	intergenic 11	daunorubicin resistance protein DrrA-family ABC transporter ATPbinding subunit (*sclA*)	B3
3,728,109	SLIV_RS 16660	substitution C→T	intergenic 15	daunorubicin resistance protein DrrA-family ABC transporter ATPbinding subunit (*sclA*)	B1
3,728,134	SLIV_RS 16660	substitution G→C	intergenic 40	daunorubicin resistance protein DrrA-family ABC transporter ATPbinding subunit (*sclA*)	B3
4,693,120	SLIV_RS 21250	insertion $C_{8\to9}$	intergenic 74	porphobilinogen synthase (*hemB*)	B4
5,121,114	SLIV_RS 22895	substitution C→A	A516D GCC→GAC	putative polysaccharide synthase (*matB*)	B1–4
7,392,037	SLIV_RS 33230	substitution A→C	V61G GTC→GGC	lipoprotein	B1
7,548,390	SLIV_RS 34020	substitution A→C	V92G GTG→GGG	nitroreductase-family deazaflavindependent oxidoreductase	B1

* The nucleotide positions and locus tags refer to the published reference genome of *S. lividans* TK24 (accession NZ_CP009124.1). Only non-silent mutations in coding sequences and mutations in intergenic sequences are shown.

+ The notation refers to the annotation of TK24-Evo strains as specified in Supplementary Table S1.

The three mutations were: (1) a single nucleotide permutation (SNP) within the coding region of transcriptional regulatory gene SLIV_RS20695; (2) a SNP in the upstream region of the adjacent gene SLIV_RS20700, which encodes an ABC transporter subunit with homology to the DrrAB transporter in the daunorubicin BGC; and (3) a frameshift mutation in the *matA* gene that is required for the production of the extracellular polysaccharide poly-β-*N*-acetylglucosamine (PNAG)[302].

S. lividans harbours a cryptic transporter that confers resistance to anthracyclines

Since two of the three mutations mapped to the same transporter locus, these were considered as primary candidates to confer anthracycline resistance in TK24-EvoA1. The transporter locus consists of a regulatory gene and two genes that encode a putative ABC transporter pair with high homology to the DrrAB transporter in the daunorubicin BGC. SLIV_RS20700 is homologous to DrrA, featuring a sequence identity of 51% with a coverage of 95% (Table 2). SLIV_RS20705 is homologous to DrrB, featuring a sequence identity of 36% with a coverage of 85% (Table 2). A putative *padR*-family transcriptional regulatory gene (SLIV_RS20695) is located immediately downstream of the transporter genes. Analysis of the TK24 genome using antiSMASH 7.0[297] indicated that the transporter genes are not part of a BGC. The genes for the putative regulator and two transporter subunits were designated *cdtR, cdtA* and *cdtB*, respectively, for **c**ryptic **d**oxorubicin **t**ransporter (Supplementary Table S4). The first mutation in TK24-EvoA1 is located in the upstream region of *cdtA*, and the second mutation is located in the coding region of *cdtR* (Table 1).

Table 2. Homology comparison between ABC transporters DrrAB, CdtAB and SclAB.

Protein pair	Identity (%)	Coverage (%)
DrrA/CdtA	51.4%	95%
DrrA/SclA	51.1%	92%
CdtA/SclA	63.0%	95%
DrrB/CdtB	35.5%	85%
DrrB/SclB	32.4%	71%
CdtB/SclB	44.1%	98%

Based on the enhanced resistance, we hypothesised that the mutations in TK24-EvoA1 led to upregulation of the transporter genes, and to enhanced export of anthracyclines. To test this hypothesis, transcriptome analysis was performed with TK24 and TK24-EvoA1. For this, TK24 and its derivative TK24-EvoA1 were grown on MM agar plates and mycelium was harvested after 24 h and 64 h (n=3). From these samples, RNA was isolated and prepared for RNA sequencing (RNAseq) analysis (see Materials & Methods for details). The data were normalised using DESeq2 v.1.34.0[303], and a Volcano plot was generated to evaluate the differentially expressed genes in TK24-EvoA1 (Figure 4A). Importantly, and in line with our hypothesis, the *cdtAB* transporter genes were significantly upregulated in the evolved strain (Figure 4B). Surprisingly, another transporter gene pair was also highly overexpressed in TK24-EvoA1 (this is worked out further below).

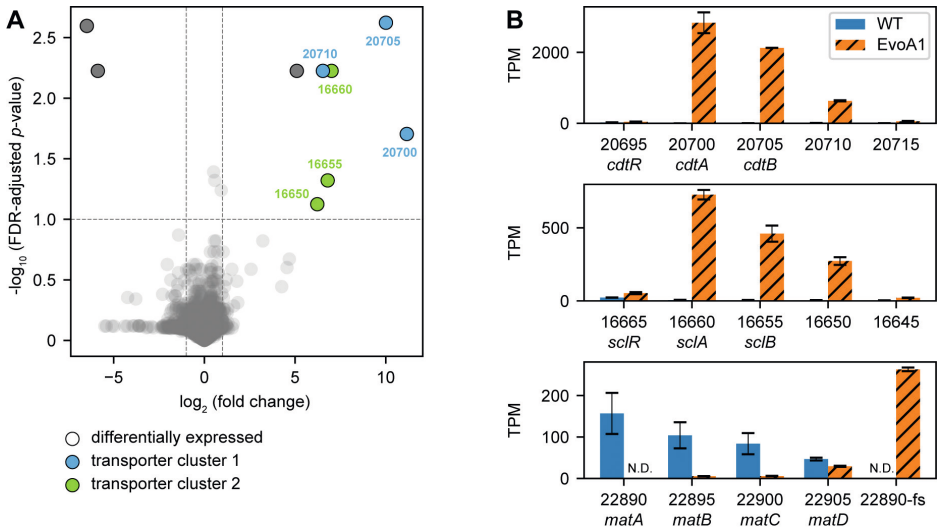

Figure 4. Changes in global gene expression in evolved strain *S. lividans* TK24-EvoA1. (A) Volcano plot of transcriptome data of TK24-EvoA1 and its parental strain grown on MM agar plates for 64 h (n=3). Genes with an FDR-adjusted p-value ‹0.1 and fold change ›2 are outlined with a black stroke. Positive $\log_2$ fold change values represent overexpression in the evolved strain. Two transporter loci exhibited significant overexpression in the evolved strain: SLIV_RS20700–20710 (highlighted in blue) and SLIV_RS16665–16650 (highlighted in green). **(B)** Bar plots of gene expression of the *cdt* locus (SLIV_RS20695–20715), the *scl* locus (SLIV_RS16665–16645), and the *mat* locus (SLIV_RS22890–22905). The bars represent the mean TPM values, and error bars indicate standard deviation (two-sample t-test, p‹0.01 for all depicted genes; N.D, not detected). Locus tags (SLIV_RS) are provided for reference (accession NZ_CP009124.1). 22890-fs indicates the *matA-matB* fusion transcript resulting from a frameshift in *matA* in TK24-EvoA1.

To investigate the role of *cdtR*, *cdtA* and *cdtB* in anthracycline resistance, we constructed deletion mutants and overexpression strains, as described below. Each strain was spotted at a concentration of $1.0 \cdot 10^4$ CFU onto SFM agar plates with increasing Doxo or DMdoxo concentrations. We aimed to constitutively express the transporter genes in TK24 to investigate whether this leads to increased resistance to Doxo and DMdoxo. To achieve this, the gene pair *cdtA-cdtB* was positioned behind the strong and constitutive *ermE** promoter[273] in the integrative vector pSET152[274]. Subsequently, the construct (pGWS1441) was introduced into TK24 via conjugation, resulting in strain MAG401 (Figure 5A). In line with the concept that the transporter may be involved in anthracycline resistance, constitutive expression of *cdtAB* in TK24 resulted in a more than eight-fold increased resistance to both Doxo (from 4 to ›64 µM) and DMdoxo (from ‹1 to 8 µM) (Figure 5C). These results show that the CdtAB transporter is involved in anthracycline resistance. However, it is important to note that the evolved strain TK24-EvoA1 exhibited resistance to more than 64 µM DMdoxo, whereas the expression construct with *cdtAB* increased DMdoxo resistance to only 8 µM. These results suggest that the transporter may not be the only resistance mechanism activated in TK24-EvoA1.

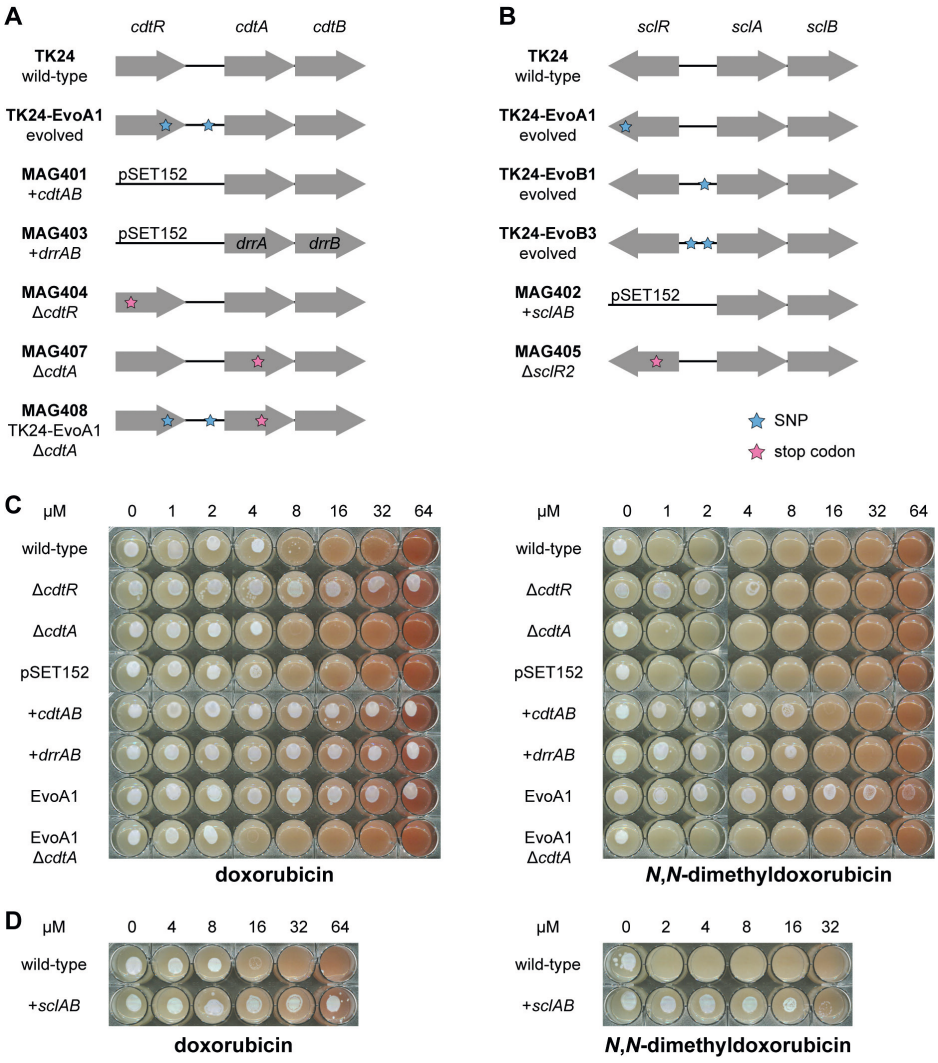

Figure 5. Activation of cryptic transporter loci *cdt* or *scl* in *S. lividans* TK24 confers resistance to Doxo and DMdoxo. Schematic representation of the strains used in this experiment related to **(A)** the *cdt* transporter locus and **(B)** the *scl* transporter locus. **(C)** S. lividans TK24 and its derivatives MAG404 (Δ*cdtR*), MAG407 (Δ*cdtA*), TK24 pSET152, MAG401 (*ermE**p-*cdtAB*), MAG403 (*ermE**p-*drrAB*), TK24-EvoA1 and MAG408 (TK24-EvoA1 Δ*cdtA*) were spotted on SFM agar plates supplemented with 1 to 64 μM Doxo or DMdoxo. For each strain, 5 μL of spore stock was spotted at a concentration of $1.0 \cdot 10^4$ CFU per spot and the plates were incubated at 30 °C for 3 days. Expression of *cdtAB* under the control of the *ermE** promoter in TK24 conferred resistance to ›64 μM Doxo and 8 μM DMdoxo. Inactivation of *cdtA* in TK24-EvoA1 rendered the strain susceptible to Doxo and DMdoxo. **(D)** TK24 and MAG402 (*ermE**p-*sclAB*) were spotted on SFM agar plates supplemented with Doxo (4–64 μM) or DMdoxo (2–32 μM). Expression of *sclAB* under the control of the *ermE** promoter in TK24 conferred resistance to ›64 μM Doxo and 16 μM DMdoxo.

Subsequently, we compared the level of resistance conferred by CdtAB of *S. lividans* with that of the Doxo transporter DrrAB originating from *S. peucetius*. To ensure maximum comparability, a similar expression construct was generated for the expression of the Doxo transporter genes *drrA-drrB* as was used for expression of the native *S. lividans* transporters genes. The construct (pGWS1443) was introduced into TK24 via conjugation, resulting in strain MAG403 (Figure 5A). Interestingly, introducing the expression constructs with *cdtAB* or *drrAB* in TK24 had the same effect. In both cases, resistance to both Doxo and DMdoxo was increased by more than eight-fold (Figure 5C).

Downstream of *cdtAB* lies *cdtR*, which encodes a putative PadR-family regulator. The gene was mutated in the evolution experiments whereas the expression of *cdtAB* was strongly upregulated. This suggests a model wherein CdtR act as a repressor of the transporter genes; if this is indeed the case, inactivation of *cdtR* in TK24 should result in upregulation of the transporter genes, leading to increased resistance. To verify that such is indeed the case, we inactivated *cdtR* via introduction of a stop codon at nucleotide position 40 (Q14*), using the CRISPR cytidine deaminase-based base editing system (CRISPR-cBEST)[304]. To do so, a *cdtR*-targeting spacer was introduced into CRISPR-cBEST construct pGWS1384. Subsequently, the resulting construct (pGWS1444) was introduced into TK24 via conjugation, resulting in strain MAG404 (Figure 5A). The successful introduction of the stop codon was confirmed by Sanger sequencing. Consistent with our hypothesis, the inactivation of *cdtR* in parental strain TK24 also resulted in increased resistance to both Doxo (from 4 µM to ›64 µM) and DMdoxo (from ‹1 µM to 4 µM) (Figure 5C). To further assess the role of the CdtAB transporter in the observed enhanced anthracycline resistance of TK24-EvoA1, we disrupted the transporter gene *cdtA* by introducing a stop codon at nucleotide position 526 (W178*). Therefore, a *cdtA*-targeting spacer was introduced into pGWS1384. Subsequently, the construct (pGWS1445) was used to create a stop codon in *cdtA* in TK24-EvoA1, resulting in strain MAG408 (Figure 5A). The inactivation of *cdtA* in the evolved strain resulted in strongly reduced resistance to both Doxo (from ›64 µM to 2 µM) and DMdoxo (from 64 µM to ‹1 µM) (Figure 5C). Similarly, *cdtA* was disrupted in TK24 (generating strain MAG407), but as expected this did not alter the already low resistance to Doxo or DMdoxo (Figure 5C).

Repeated evolution experiment reveals mutations in a second transporter locus

SNP analysis of TK24-EvoA1 revealed mutations that led to the activation of the transporter gene pair *cdtAB*. However, transcriptome data showed that a second transporter gene pair was also upregulated in the Doxo resistant mutant (Figure 4). This second transporter locus consists of a regulatory gene (*sclR*) and two genes (*sclAB*) that encode another ABC transporter pair with high homology to the DrrAB transporter in the daunorubicin BGC (Supplementary Table S4)[305]. SclA (SLIV_RS16660) is homologous to DrrA with an aa sequence identity of 51% with a coverage of 92% (Table 2). SclB (SLIV_RS16655) is homologous to DrrB, featuring an aa sequence identity of 32% with a coverage of 71% (Table 2). A *tetR*-family transcriptional regulatory gene (*sclR*, SLIV_RS16665) is located downstream of these transporter genes. Prior

research in *S. coelicolor* demonstrated that SCO4358 (an ortholog of SclR) acts as a repressor of SCO4359–4360 (encoding a SclAB ortholog), while the transporter acts as a multidrug transporter[305]. Interestingly, deletion of *sclR* in *S. coelicolor* resulted in about two-fold enhanced resistance to daunorubicin[305]. We were therefore curious if SclAB was also involved in the Doxo and DMdoxo resistance of TK24-EvoA1.

Upon further investigation of this genomic region in TK24-EvoA1, a partial mutation was identified in *sclR* resulting in an amino acid change (L242R). The mutation was detected in 41% of the Illumina reads. Sanger sequencing of PCR products of 15 single colonies indicated that the mutation was present in three out of 15 colonies. Interestingly, when we repeated the evolution experiment and performed SNP analysis on four additional anthracycline-resistant mutants (TK24-EvoB1-B4), we also identified mutations in the *scl* transporter locus. In TK24 evolution line B, three distinct mutations were located in the promoter region of *sclA*, of which one mutation occurred in TK24-EvoB1 and two mutations in TK24-EvoB3 (Table 1).

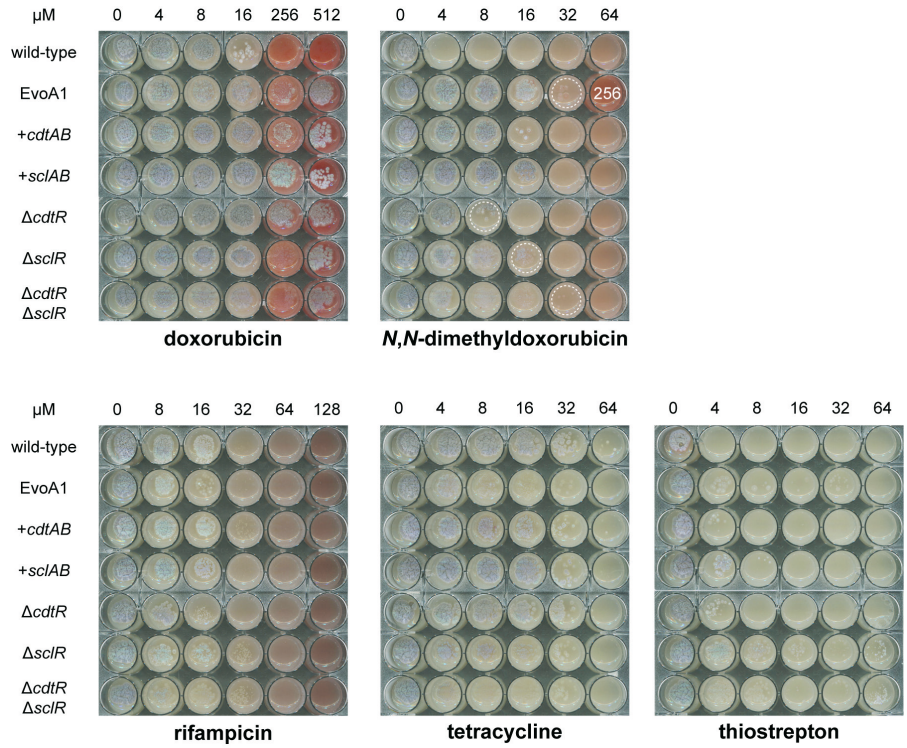

Figure 6. Role of CdtAB and SclAB transporters in resistance against different antibiotics. *S. lividans* TK24 and its derivatives MAG401 (*ermE**p-*cdtAB*), MAG402 (*ermE**p-*sclAB*), MAG404 (Δ*cdtR*), MAG405 (Δ*sclR*) and MAG406 (Δ*cdtR*Δ*sclR*) were spotted onto SFM agar plates supplemented with Doxo (4–512 μM), DMdoxo (4–64 μM), rifampicin (8–64 μM), tetracycline (4–64 μM) or thiostrepton (8–64 μM). For each strain, 5 μL of spore stock was spotted at a concentration of $1.0 \cdot 10^4$ CFU per spot and the plates were incubated at 30 °C for 6 days. Dashed circles indicate the highest concentration that allows growth. In one well, a final concentration of 256 μM DMdoxo was added, which is indicated.

The other two isolates from this evolution line did not have mutations in either the *scl* or *cdt* locus. We constructed an overexpression strain to study the effect of the SclAB transporter on Doxo and DMdoxo resistance. The gene pair *sclA-sclB* was positioned behind the strong and constitutive *ermE** promoter in the integrative vector pSET152. The construct (pGWS1442) was then introduced into TK24 via conjugation, resulting in strain MAG402 (Figure 5B). The recombinant strain showed enhanced resistance to both Doxo (from 8 to ›64 µM) and DMdoxo (from ‹2 to 16 µM) (Figure 5D). This indicates that the SclAB transporter can provide strong resistance to Doxo and DMdoxo.

Taken together, these data suggests that both transporter pairs CdtAB and SclAB can provide significant resistance to anthracyclines. While expression of either *cdtAB* or *sclAB* under the control of the *ermE** promoter resulted in increased Doxo and DMdoxo resistance, it was insufficient to reach the same levels of resistance as the evolved strain TK24-EvoA1. To test whether the co-expression of both transporters further increased resistance, a derivative of TK24 was created wherein both *cdtR* and *sclR* were inactivated. Using the same strategy as for the other mutants, strain TK24 Δ*cdtR*Δ*sclR* was created and designated MAG406. We also created the single mutant TK24 Δ*sclR* as control, which was designated MAG405. The Doxo and DMdoxo resistance of the single and double mutants was evaluated. All mutants were resistant to at least 512 µM Doxo (Figure 6). However, a difference between the two transporters could be observed with DMdoxo. Strains expressing *cdtAB* could grow with up to 8 µM DMdoxo, whereas the strains expressing *cdtAB* could grow with two-fold more DMdoxo (Figure 6). Interestingly, the double mutant of *cdtR* and *sclR* could grow with up to 32 µM DMdoxo, similar as the evolved strain TK24-EvoA1 (Figure 6).

CdtAB and SclAB exhibit specificity for anthracyclines

Transporters CdtAB and SclAB both provided significant resistance to anthracyclines. To investigate the specificity of the two cryptic transporters, the resistance to other classes of antibiotics was also evaluated. Antibiotics that were tested were rifampicin, tetracycline and thiostrepton, besides Doxo and DMdoxo. Tetracycline is a tetracyclic aromatic polyketide that is structurally related to Doxo, and which like Doxo is a DNA-targeting antibiotic. Rifampicin targets RNA polymerase, whereas thiostrepton is an oligopeptide that targets the ribosome. We tested the panel of antibiotics against *S. lividans* TK24, and its derivatives TK24-EvoA1, MAG401 (*ermE**p-*cdtAB*), MAG402 (*ermE**p-*sclAB*), MAG404 (Δ*cdtR*), MAG405 (Δ*sclR*) and MAG406 (Δ*cdtR*Δ*sclR*). The evolved strain TK24-EvoA1 did not exhibit increased resistance to rifampicin or tetracycline as compared to the parental strain (Figure 6). The mutant strains exhibited various levels of resistance to rifampicin and tetracycline, but never more than a two-fold difference as compared to the parental strain (Figure 6). More variety in resistance to thiostrepton was observed. Strains expressing *sclAB* (MAG402, MAG405 and MAG406) showed higher resistance to thiostrepton than the parental strain. However, growth and development of the mutants was inhibited at the low concentration of 4 µM thiostrepton, whereas the mutant strains grew at very high concentrations of Doxo (up to 512 µM).

N,N-dimethyldoxorubicin resistant mutants also harbour SNPs in the *mat* locus

In TK24 evolution line A only three mutations were found, two SNPs in the *cdt* locus and a frameshift mutation in *matA* (SLIV_RS22890). The frameshift mutation within the coding region of *matA* in TK24-EvoA1 resulted in an in-frame fusion of *matA* and *matB* (Table 1, Figure 4). Importantly, we found a SNP in *matB* (SLIV_RS22895) in all isolates of TK24 evolution line B that resulted in an A516D substitution in MatB (Table 1). MatAB are an enzyme couple that produces the extracellular polysaccharide poly-β-*N*-acetylglucosamine (PNAG), which acts as a sticky polymer that 'glues' hyphae together, leading to pellet formation in submerged cultures[302,306]. Inactivation of *matAB* in *S. lividans* results in loss of PNAG production and thus fragmented growth, as well as increased growth rate[302,306].

To evaluate the effect of the mutations within the *mat* locus of TK24 on both morphology and resistance to DMdoxo, the evolved isolates were grown in submerged TSB cultures (Figure 7A). All evolved isolates exhibited more fragmented growth with smaller pellets compared to the parental strain. Given the similarity in phenotypes among the evolved strains, we used TK24-EvoA1 as representative strain to investigate the impact of the *mat* mutations on DMdoxo resistance. The impact of the altered morphology of the evolved strains on DMdoxo resistance was studied by microtiter plate (MTP) cultivation in a BioLector system. This automated cultivation device provides non-invasive measurements of biomass concentration based on back-scattered light. For each strain, $1.0 \cdot 10^6$ CFU·mL^{-1} pregerminated spores were inoculated in 1 mL of TSB medium with increasing DMdoxo concentrations. Biomass measurements were taken at a 15-min interval. This method was applied to evaluate the DMdoxo resistance of TK24-EvoA1 and its parent *S. lividans* TK24 in a submerged environment. Additionally, a *matAB* deletion mutant of *S. lividans* 1326[306] and its parent were evaluated using the same method. *S. lividans* 1326 is a closely related strain to TK24 that carries two genomic plasmids. The *matAB* deletion mutant (GAD05) enabled the evaluation of how morphology affects anthracycline resistance, independent of other mutations.

As expected, TK24-EvoA1 demonstrated accelerated growth compared to the parental strain, demonstrated by the steeper growth curve and higher biomass concentration (Figure 7B). *S. lividans* TK24 exhibited growth inhibition at 0.5 µM DMdoxo and complete growth arrest at 2 µM DMdoxo. TK24-EvoA1 demonstrated improved resistance, with growth inhibition only beginning to be observed at 16 µM DMdoxo and growth was still observed at the highest tested concentration of 32 µM DMdoxo (Figure 7B). While *S. lividans* 1326 Δ*matAB* also exhibited faster growth than the parental strain, the mutant did not show higher resistance to DMdoxo, with both parent and mutant being fully inhibited by concentrations as low as 1 µM DMdoxo. These observations collectively suggest that while fragmented morphology is associated with an increased growth rate, it does not directly influence resistance to DMdoxo.

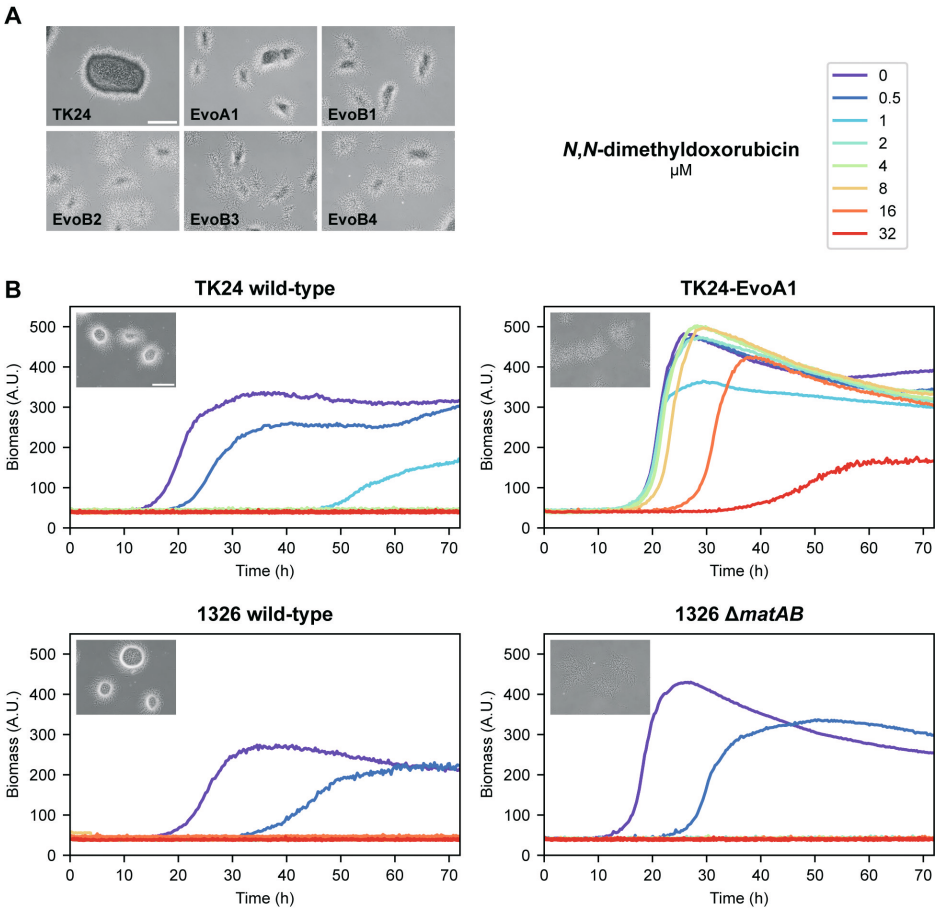

Figure 7. Inactivation of *matAB* does not directly affect DMdoxo resistance. (A) *S. lividans* TK24 and five evolved isolates were cultivated in TSB medium in shake flasks for 24 h. All evolved isolates exhibited a more fragmented morphology compared to the parental strain. Scale bar: 200 µm. **(B)** *S. lividans* strains TK24, TK24-EvoA1, 1326 and 1326 Δ*matAB* were cultivated in 1 mL of TSB medium with 0.5 to 32 µM DMdoxo in the BioLector. TK24-EvoA1 demonstrated uninhibited growth up to 8 µM DMdoxo, while TK24, 1326 and 1326 Δ*matAB* were already significantly inhibited by 0.5 µM DMdoxo. Deletion of *matAB* in *S. lividans* 1326 creased the growth rate but did not directly affect resistance to DMdoxo. Scale bar: 200 µm.

Evolution of *S. peucetius* to *N,N*-dimethyldoxorubicin generates mutations in *fusA*

Next, we explored the evolved isolates of *S. peucetius* with enhanced resistance to Doxo and DMdoxo. For *S. peucetius* we sequenced single colony isolates from two parallel evolution lines, which were designated "*S. peucetius*-EvoAx" and "*S. peucetius*-EvoBx" (Supplementary Table S1). Three single colony isolates were sequenced from evolution line A and four from evolution line B. Whole-genome sequencing and genomic variant detection was performed similarly as for TK24. The genome of the parental strain was used as a reference to filter out all changes relative to the published genome of *S. peucetius* var. *caesius* ATCC 27952 (accession

NZ_CP022438.1). After filtering the data, a total of 16 distinct mutations were identified across all the *S. peucetius* evolved isolates (Table 3). These mutations included single nucleotide polymorphisms (SNPs), as well as insertions, deletions or substitutions of short sequences (up to 13 base pairs).

Table 3. Genomic variants identified in *S. peucetius* isolates from evolution experiments with DMdoxo.

Position*	Locus tag*	Variants	Annotation	Description	Isolate+
Genomic variants detected in evolution line A					
1,524,293	CGZ69_ RS07190	deletion Δ12 bp	ΔPTPV 7–18/1368 nt	MHS family MFS transporter	A1–3
1,535,150	CGZ69_ RS07230	deletion $G_{6\rightarrow5}$	frameshift 248/2262 nt	molybdopterindependent oxidoreductase	A1–3
2,186,646	CGZ69_ RS10020	substitution G→T	Y332* TAC→TAA	Z1 domaincontaining protein	A1–3
2,610,861	CGZ69_ RS12060	insertion $C_{6\rightarrow7}$	intergenic 200	CYTH and CHAD domaincontaining protein	A2–3
4,422,376	CGZ69_ RS20380	deletion Δ13 bp	intergenic 351	sigma70 family RNA polymerase sigma factor	A1–3
4,584,873	CGZ69_ RS21225	insertion $C_{6\rightarrow7}$	frameshift 883/2127 nt	elongation factor G (*fusA*)	A1–3
5,014,608	CGZ69_ RS23245	substitution G→A	intergenic 51	ABC transporter substratebinding protein	A1–3
5,280,211	CGZ69_ RS24490	substitution GT→CC	V422P GTC→CCC	excinuclease ABC subunit UvrA (*drrC*)	A1–3
5,777,792	CGZ69_ RS26780	substitution T→C	L925P CTC→CCC	translation initiation factor IF2 (*infB*)	A1–3
5,915,471	CGZ69_ RS27320	substitution G→A	A3089T GCC→ACC	nonribosomal peptide synthetase	A2–3
7,182,877	CGZ69_ RS32420	substitution C→A	P81H CCT→CAT	DUF4012 domaincontaining protein	A1–3
Genomic variants detected in evolution line B					
1,042,186	CGZ69_ RS04840	substitution G→T	intergenic 1	SDR family NAD(P)dependent oxidoreductase	B1–4
1,992,539	CGZ69_ RS09140	insertion $C_{6\rightarrow5}$	frameshift 923/957 nt	16S rRNA (cytosine(1402) N(4))methyltransferase (*rsmH*)	B1, B4
2,147,743	CGZ69_ RS09835	substitution G→A	T76M ACG→ATG	endonuclease/exonuclease/phosphatase family protein	B1–4
2,184,740	CGZ69_ RS10015	substitution T→G	H38P CAC→CCC	PD(D/E)XK motif protein	B1–4
4,585,095	CGZ69_ RS21225	deletion Δ1 bp)	frameshift 1105/2127 nt	elongation factor G (*fusA*)	B2–3

* The nucleotide positions and locus tags refer to the published reference genome of *S. peucetius* var. *caesius* ATCC 27952 (accession NZ_CP022438.1). Only non-silent mutations in coding sequences and mutations in intergenic sequences are shown.

+ The notation refers to the annotation of *S. peucetius*-Evo strains as specified in Supplementary Table S1.

A few mutations stood out (Table 3). Firstly, only one mutation was identified within the daunorubicin BGC. All isolates from evolution line A harboured a mutation in *drrC* (CGZ69_RS24490), resulting in a V422P amino acid substitution. DrrC is an UvrA-like protein that is involved in DNA repair[68]. Furthermore, two mutations were identified in separate transporter loci. The first SNP was located within the promoter region of an ABC transporter gene (CGZ69_RS23245), and was found in all isolates from evolution line A. Secondly, all isolates from this evolution line also harboured a 12-base pair deletion at the beginning of a major facilitator superfamily (MFS) transporter gene (CGZ69_RS07190). Furthermore, two distinct mutations occurred in parallel in both evolution lines resulting in frameshift mutations in *fusA*, a gene that encodes elongation factor G in *Streptomyces*[307]. This gene is widely conserved and is an essential factor for ribosome translocation and recycling[307]. Fusidic acid is an inhibitor of *fusA*, and inactivation of *fusA* results in fusidic acid resistance.

Anthracycline resistance mechanisms and BGC distribution in streptomycetes

The two cryptic transporters CdtAB and SclAB conferred significant resistance to both Doxo and DMdoxo in TK24. Preliminary findings suggested a specific affinity of these transporters for anthracyclines. This observation prompted the question why TK24 harbours two distinct transporters for this class of compounds, and whether these transporters are present in other streptomycetes. It is plausible that these transporters have evolved due to the abundant presence of anthracyclines in their environment. To date, only 13 anthracycline BGCs have been identified[266], but it is unknown how many streptomycetes can produce anthracyclines. Therefore, we analysed 629 complete genome sequences of Streptomycetaceae for the presence of putative anthracycline BGCs and CdtAB or SclAB homologs.

To explore the prevalence of anthracycline BGCs, we developed a custom detection rule using the antiSMASH 7.0 framework[297] based on two criteria. First, the standard type II polyketide synthase (T2PKS) detection rule of antiSMASH was used to identify clusters that encode aromatic polyketides. This rule checks for the presence of the ketosynthase subunits (KS_α/KS_β) of the minimal PKS, and predicts the product class based on KS_β and cyclases in the cluster[308]. To refine the detection for anthracycline BGCs, we introduced a second criteria based on the glycosyltransferases and P450 auxiliary enzymes of known anthracycline BGCs[266]. We manually searched for genes for DnrS (glycosyltransferase) and DnrQ (auxiliary enzyme) homologs in the thirteen known anthracycline BGCs using pBLAST, and constructed profile hidden Markov models (pHMM). A positive hit was determined when either a DnrS or a DnrQ homolog was predicted by be encoded by a T2PKS cluster. Cut-off values were determined using positive controls (known anthracycline BGCs) and negative controls (angucycline BGCs from the MIBiG database[298]). Of the 629 genomes in our study, 5% harboured a putative anthracycline BGC based on our criteria (Supplementary Table S9). The BGCs were manually curated by comparison to known anthracycline BGCs. Most clusters showed high similarity with known anthracycline BGCs, of which aclarubicin (nine clusters) and Doxo (six clusters) were the most abundant. Five clusters exhibited low similarity to known anthracycline BGCs.

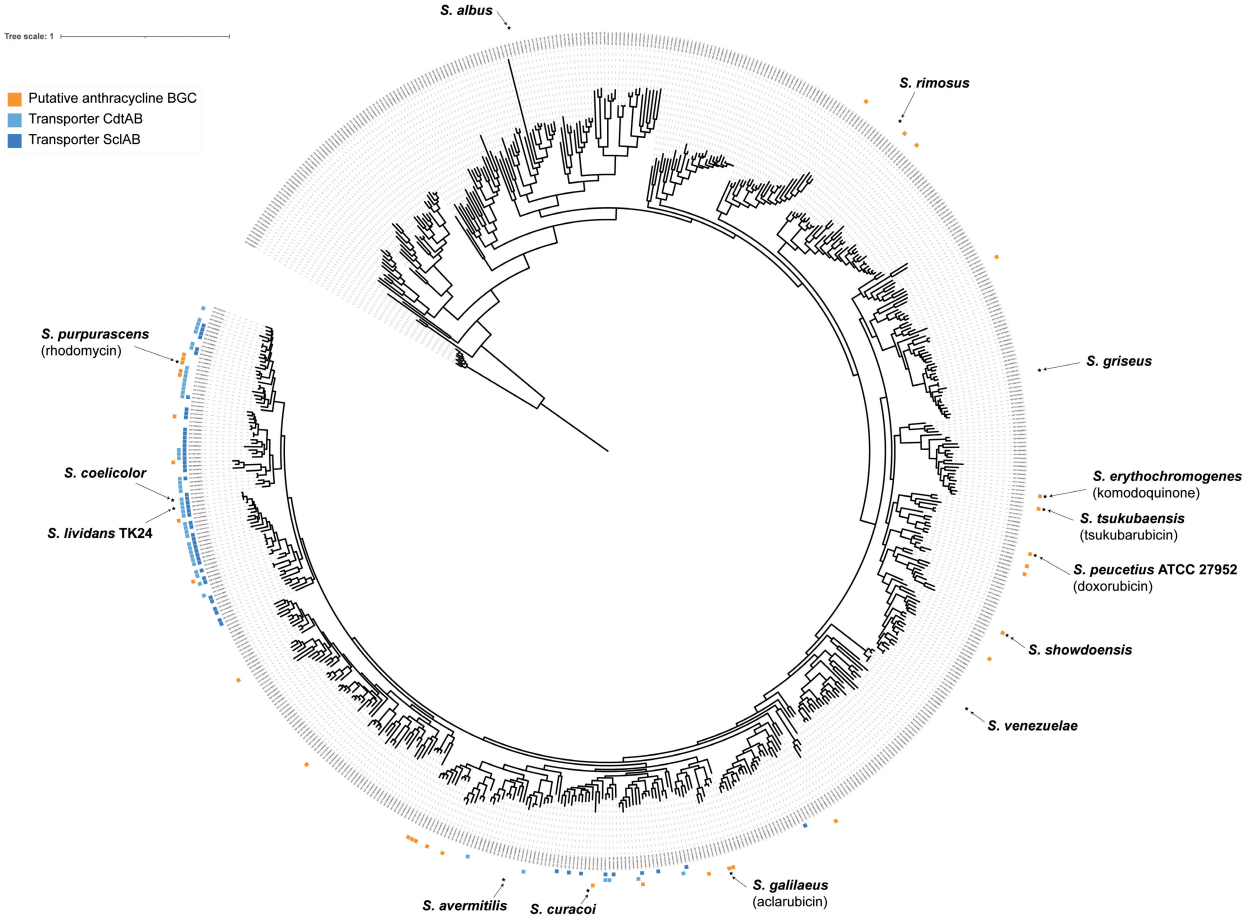

Figure 8. Distribution of CdtAB and SclAB transporters and correlation to putative anthracycline BGCs in actinomycetes. A maximum likelihood phylogenetic tree was generated using 629 *Streptomycetaceae* genomes and eight reference *Oerskovia* species as outgroup obtained from the NCBI RefSeq database. The outer ring indicates strains containing a putative anthracycline BGC (in orange). The middle ring indicates strains that harbour a CdtAB homolog (in light blue), and the inner ring indicates the presence of a SclAB homolog (in dark blue). Known anthracycline producers, *Streptomyces* model strains, and other strains described in this study are indicated.

Subsequently, a detection rule was designed for the presence of transporters encoded by *cdtAB* and *sclAB* using 100 proteins homologous to SCO3417–3418 (orthologs of CdtAB) and SCO4359–4360 (orthologs of SclAB) of *S. coelicolor*. Out of the 629 genomes, 12% yielded a transporter homologous to either CdtAB or SclAB, with 4% of the genomes harbouring both types of transporters. Subsequently, we studied the phylogenetic relationship between the presence of an anthracycline BGC and the CdtAB and SclAB homologs. A maximum likelihood phylogenetic tree was constructed based on the 629 genome sequences. The genomes harbouring a putative anthracycline BGC were scattered across the phylogenetic tree (Figure 8). In contrast, genomes harbouring homologs of CdtAB and SclAB clustered in two distinct groups on the phylogenetic tree. Unsurprisingly, the majority of the transporters were detected in genomes closely related to *S. lividans* (Figure 8). Only six strains were found to simultaneously harbour a putative anthracycline BGC and one of the transporter loci elsewhere in the genome. All putative anthracycline BGCs harboured an ABC or MFS transporter, but these transporters were not closely related to CdtAB or SclAB.

Discussion

Anthracyclines are anticancer drugs that are widely used in the clinic. At the same time, anthracyclines also have antibiotic activity, and exhibit strong toxicity against a wide range of bacteria, including those that produce them. The Doxo-producer *S. peucetius* var. *caesius* is much more sensitive to DMdoxo compared to Doxo (Figure 1). This finding prompted further studies into anthracycline resistance mechanisms within actinomycetes. Screening of our in-house collection of actinomycetes revealed that while the strains exhibited varying sensitivity to Doxo, they were all highly sensitive to DMdoxo. This high sensitivity to DMdoxo was harnessed to conduct adaptive laboratory evolution of *S. lividans* TK24, which resulted in the activation of two cryptic transporters conferred significant resistance to anthracyclines. Constitutive expression of either of these transporters in the parental strain resulted in more than eight-fold increased resistance to both Doxo and DMdoxo.

Analysis of spontaneous mutants of *S. lividans* TK24 with enhanced resistance to DMdoxo revealed the transcriptional activation of two homologous ABC transporters. The expression of *cdtAB* is controlled by the downstream gene encoding a putative PadR-like transcriptional regulator, CdtR. The PadR-family represents a large, diverse, and relatively underexplored protein family among the one-component signal transduction systems. The archetypal PadR acts as a repressor of phenolic acid decarboxylates in Gram-positive bacteria[309]. Various members of the PadR family control the expression of multidrug efflux pumps. For example, LmrR controls the expression of *lmrCD*, encoding a major multidrug ABC transporter in *Lactococcus lactis*[310]. Similarly, LadR controls the expression of *mdrL*, encoding a multidrug MFS efflux pump[311]. Directed inactivation of *cdtR* via the introduction of a stop codon resulted in a phenotype similar to constitutive expression of *cdtAB*, implying that CdtR represses the transcription of *cdtAB*. PadR regulators are generally inactivated via the binding to ligands. In the case of CdtR, the

accumulation of spontaneous mutations activated the transcription of *cdtAB*. Anthracyclines did not elicit anthracycline resistance, and it is yet unknown what the ligand is for CdtR.

The second transporter, SclAB, is controlled by a TetR-like transcriptional regulator, SclR. The TetR family of transcriptional regulators is extensively characterised and is widely associated with antibiotic resistance and the regulation of genes encoding small-molecule transporters[312]. Prior research demonstrated that inactivation of *sclR* in *S. lividans* provides resistance to various compounds, including the macrolide spiramycin, daunorubicin and ethidium bromide[305]. Further studies also revealed a role of SclAB in resistance against the acyldepsipeptides, which are also macrolide antibiotics[313]. *S. coelicolor* harbours three TetR-regulated ABC-family transporters (see Supplemental Table S4)[305]. Deletion of each TetR regulatory gene (SCO1718, SCO4357 and SCO5384) resulted in increased production of actinorhodin and undecylprodigiosin, as well as mild resistance to different classes of antibiotics[305]. Deletion of SCO4358 (an ortholog of *sclR*) in *S. coelicolor* increased daunorubicin resistance from 6 $\mu g \cdot mL^{-1}$ to 10 $\mu g \cdot mL^{-1}$, which is much less than we observed for the *sclR* deletion mutant in TK24.

Our work indicates that both CdtAB and SclAB provide particularly strong resistance to anthracyclines. When we introduced expression cassettes containing *cdtAB* or *sclAB*, or disrupted *cdtR* or *sclR*, a more than eight-fold increase in resistance was observed to both Doxo and the stronger antibiotic DMdoxo. However, only a marginal increase in resistance was seen for the other antibiotics tested. This suggests that the transporters preferentially provide resistance to anthracyclines over other tetracyclic polyketides. This interpretation is further supported by the observation that the enhanced expression of these transporters offers a level of resistance comparable to that of the Doxo transporter, DrrAB. Both CdtAB and SclAB transporters are homologs of DrrAB, with CdtA and SclA share 51.4 and 51.1% sequence identity with DrrA, respectively. The two *S. lividans* transporters CdtA and SclA share 63.0% sequence identity (Table 2). This preliminary data suggests that both two transporters exhibit specificity for anthracyclines, although further studies should be performed to confirm this.

In addition to mutations in the two transporter loci, mutations were identified in the *mat* locus in the two parallel evolution lines of *S. lividans* TK24. These genes are involved in the biosynthesis of the exopolysaccharide PNAG, which forms a layer that covers the vegetative hyphae[302,306]. Originally discovered in a high-dilution rate chemostat evolution experiment, their inactivation might confer growth advantages in our evolution experiment with serial batch cultivation, where strains grow at the maximum growth rate[314]. Our results indicate that the mutations in the *mat* locus did not directly affect Doxo resistance; however, the positive effect of the deletion of *matAB* on the growth rate may have facilitated resistance development.

An important question is why *S. lividans* TK24 harbours two cryptic transporters that provide resistance to anthracyclines. In their natural environments, streptomycetes are confronted with a diverse array of natural products produced by other species[51,315]. To survive in such hostile environments, streptomycetes not only produce a diverse array of natural products,

but also acquire or evolve highly specific resistance elements against exogenous antibiotics[316]. Consequently, many streptomycetes harbour resistance mechanisms against multiple classes of antibiotics[317]. For example, the model organism *S. coelicolor* harbours specific resistance genes against vancomycin and chloramphenicol, which it does not produce itself. Two MFS efflux pumps (SCO7526 and SCO7662) provide chloramphenicol resistance, and the corresponding genes are constitutively expressed even in absence of chloramphenicol[318]. The vancomycin resistance cassette is regulated by a two-component system involving VanR and VanS, and is activated in presence of vancomycin[319,320]. Interestingly, in contrast to the chloramphenicol and vancomycin resistance mechanisms, the *cdtAB* and *sclAB* gene pairs were silent under the tested growth conditions, even in the presence of anthracyclines. The only way to activate the genes was by evolving resistant colonies by challenging *S. lividans* TK24 with high concentrations of DMdoxo. Our results show that apart from cryptic BGCs encoding undiscovered natural products, *Streptomyces* genomes also contain cryptic resistance mechanisms. This suggests that these organisms may hold a reservoir of untapped genetic potential, both in terms of antibiotic production and resistance mechanisms. It is important to note that antibiotic resistance often comes at a cost, with mutants typically showing reduced fitness[321,322], and we cannot rule out that the same holds for anthracycline resistance.

Bioinformatics analysis revealed the presence of genes encoding close homologs of the CdtAB and SclAB transporters in 12% of Streptomycetaceae reference genomes. Considering this high frequency of occurrence, we expect that their silence may be conditional; in other words, in nature these genes may be activated by an environmental signal. Alternatively, activation of the transporters may require random mutations that occur occasionally within a colony, resulting in resistance in a small part of the population. Some 5% of the selected actinomycete genomes contain a putative anthracycline BGC. This finding aligns with prior research that identified daunorubicin-like BGCs in 3.6% of 1110 selected *Streptomyces* genomes[168]. Thus, the existence of anthracycline transporters may be explained by the frequent occurrence of Actinobacteria that produce anthracyclines. The presence of anthracycline BGCs did not correlate with the presence of the transporter genes. Only six genomes were found to simultaneously harbour an anthracycline BGC and one of the transporter loci elsewhere in the genome. This suggests that the CdtAB and SclAB transporters function as a resistance mechanism against anthracyclines in the environment.

Self-resistance mechanisms against toxic natural products such as anthracyclines are typically encoded within the BGCs[57,323]. In the case of the CdtAB and SclAB transporters we failed to detect a direct correlation with anthracycline BGCs, suggesting that anthracycline resistance may be a more general trait of Actinobacteria. In addition, it should be noted that we identified wild-type streptomycetes with high resistance to anthracyclines but which lacked genes for the two transporters and anthracycline BGCs, and that we obtained spontaneous anthracycline-resistant mutants of *S. lividans* (line B) that exhibited strong resistance, but did not show enhanced expression of either of the transporter loci. These results suggest that actinomycetes harbour additional yet unidentified anthracycline resistance mechanisms. *S. venezuelae*

and *S. rimosus* showed surprisingly high resistance to Doxo, but neither strain harboured a putative anthracycline BGC or CdtAB-like and SclAB-like transporters in their genomes. We hypothesised that the jadomycin BGC in *S. venezuelae* may be involved in Doxo resistance, because of their structural similarities. However, deletion of the jadomycin BGC in *S. venezuelae* did not affect resistance to Doxo. Thus, another anthracycline resistance mechanism must be operational. Screening of our MBT collection of Actinobacteria revealed that a substantial number of actinomycetes exhibited resistance to relatively high concentrations of Doxo, whereby a spectrum of resistance levels was observed, with some strains growing at concentrations exceeding 200 µM. Some strains failed to develop in the presence of anthracyclines, while others were unaffected and developed aerial hyphae even at the highest tested concentrations. Els4, Hm84 and MBT74 demonstrated significant resistance to Doxo. Like in *S. venezuelae*, no putative anthracycline BGC or CdtAB-like and SclAB-like transporters were detected in their genomes, again suggesting alternative mechanisms of anthracycline resistance.

In the DMdoxo-evolved *S. peucetius* isolates, two distinct frameshift mutations occurred in the parallel evolution lines in *fusA*. The gene encodes elongation factor G, which is widely conserved and is an essential factor for ribosome translocation and recycling[307]. Elongation factor G is the target of fusidic acid, and mutations in *fusA* occur spontaneously in presence of fusidic acid. We are currently investigating whether these mutations are responsible for the increased anthracycline resistance of the *S. peucetius* isolates.

Interestingly, a DMdoxo-evolved isolate of *S. showdoensis* was exceptionally resistant to both Doxo and DMdoxo, and the mutation did not noticeably alter growth or development of the strain. No CdtAB-like and SclAB-like transporters could be detected within the *S. showdoensis* genome, but we detected a putative anthracycline BGC. The most closely related BGCs are those that encode the biosynthesis of komodoquinone (MiBIG cluster BGC0001815, 65% similarity) and of cinerubin B (MiBIG cluster BGC0000212, 57% similarity)[298]. The BGC contains a putative ABC transporter, which could be responsible for the strong anthracycline resistance of this strain but warrants further investigation.

In conclusion, our findings revealed the presence of anthracycline transporters within actinomycetes that do not produce anthracyclines themselves. Furthermore, our results show that additional resistance mechanisms remain to be identified in other anthracycline resistance strains. These results indicated that cryptic resistance mechanisms can be activated upon prolonged exposure to toxic compounds.

Materials and Methods

Bacterial strains and growth conditions

The bacterial strains used in this work are listed in Supplementary Table S1. *E. coli* strains JM109[281] and ET12567 harbouring pUZ8002[282] were used for routine cloning and conjugation of

plasmids to *Streptomyces*, respectively. *E. coli* strains were cultivated at 37 °C on Luria-Bertani (LB) agar plates or in LB medium supplemented with the appropriate antibiotics.

Strains *S. coelicolor* A3(2), *S. coelicolor* M145, *S. lividans* 1326 and *S. lividans* TK24[1] were obtained from the John Innes Centre strain collection. *Streptomyces* strains *S. peucetius* var. *caesius* ATCC 27952, *S. galilaeus* ATCC 31615, *S. venezuelae* ATCC 10712 and *S. rimosus* ATCC 10970, *S. showdoensis* ATCC 15227 and *S. curacoi* DSM 40107 were obtained from the DSMZ strain collection. Other strains were obtained from the Leiden University strain collection, consisting of strains previously isolated from soil samples of Qinling Mountains, Shanxi province, China from the Himalaya mountain range in Nepal or from Dutch dune soil[294], from a wastewater treatment plant[295] or from sponges[296].

All media and routine *Streptomyces* techniques have been described previously[1]. Soy flour mannitol (SFM) agar plates were used for the collection of spores, conjugation experiments and phenotypical characterisation. Tryptone soy broth (TSB) was used for liquid cultivation of *Streptomyces* strains. The growth media were supplemented with 20 $\mu g \cdot mL^{-1}$ thiostrepton when required. Cultures were grown in a total volume of 20 mL of liquid medium in 100 mL Erlenmeyer flasks equipped with metal coils. Shake flasks were incubated in an orbital shaker with a 2-inch orbit at 200 rpm at 30 °C. In cases of poor sporulation, mycelial stocks were prepared as an alternative to spore stocks. Strains were cultivated in TSB medium for 2 days, the biomass was washed with 10.3% (w/v) sucrose, resuspended in 20% (w/v) glycerol, and stored at -80 °C. To study the morphology of *Streptomyces* strains in liquid environments, strains were cultivated in TSB medium without metal coils, and imaged using a Zeiss Axio Lab A1 upright microscope equipped with an Axiocam MRc camera.

Construction of plasmids and strains

All plasmids described in this work are listed in Supplementary Table S2 and oligonucleotides in Supplementary Table S3. Plasmid maps were generated using SnapGene 6.0 (Supplementary Figure S1).

Constructs for expression of transporter genes

For the expression of biosynthetic genes, the integrative vector pSET152[274] was employed. pSET152 integrates into the attachment sites within the *Streptomyces* genome for bacteriophage φC31 and harbours an apramycin resistance cassette.

To generate a construct for expression of *cdtA* (SLIV_RS20700) and *cdtB* (SLIV_RS20705) from *Streptomyces lividans* TK24 (Supplementary Table S4), the coding sequence (+0/+1782 relative to the start codon of *cdtA*) was amplified by primers MH401/MH402 from genomic DNA and digested using NdeI/XbaI. A DNA fragment containing the *ermE** promoter[273] was digested from pHM10a[324] using EcoRI/NdeI. The two DNA fragments were simultaneously cloned into EcoRI/XbaI-digested pSET152 to generate pGWS1441.

To generate a construct for expression of *sclA* (SLIV_RS16660) and *sclB* (SLIV_RS16655) from *S. lividans* TK24 (Supplementary Table S4), the coding sequence (+0/+1906 relative to the start codon of *sclA*) was amplified by primers MH403/MH404 from genomic DNA. A DNA fragment containing the pSET152 backbone and the *ermE** promoter was excised from pGWS1441 using NdeI/XbaI. The coding sequence of *sclAB* was cloned into linearised *ermE**p::pSET152 via Gibson assembly[277] to generate pGWS1442. To generate a construct for expression of *drrA* and *drrB* from *Streptomyces peucetius* var. *caesius* ATCC 27952 (further referred to as *S. peucetius*, Supplementary Table S4), the coding sequence (+0/+1897 relative to the start codon of *drrA*) was amplified by primers MH405/MH406 from *S. peucetius* genomic DNA and digested using NdeI/XbaI. A DNA fragment containing the pSET152 backbone and the *ermE** promoter was excised from pGWS1441 using NdeI/XbaI. The PCR product containing *drrAB* was cloned into *ermE**p::pSET152 to generate pGWS1443.

Constructs for gene disruption

The CRISPR cytidine deaminase-based base editing system (CRISPR-cBEST) was employed for gene disruption[304]. Firstly, the *tipA* promoter in pCRISPR-cBEST[304] was replaced with the *gapdh* promoter. Therefore, a fragment containing the *ermE** promoter, a sgRNA scaffold and the *gapdh* promoter was digested from the previously published construct pGWS1370[325] using NcoI/NdeI, and subsequently cloned into pCRISPR-cBEST to generate pGWS1384. Consequently, the expression of Cas9 nickase (D10A), APOBEC-1 (cytidine deaminase) and UGI (uracil-DNA glycosylase inhibitor) within pGWS1384 was regulated by the *gapdh* promoter instead of the *tipA* promoter.

Inactivation of *cdtR* (SLIV_RS20695) was achieved by creating a stop codon at nucleotide position 40 (Q14*). A *cdtR*-targeting spacer was introduced into NcoI-linearised pGWS1384 via Gibson assembly[277] using the bridging oligonucleotide MH407, generating pGWS1444. Similarly, to inactivate *cdtA* (SLIV_RS20700) by creating a stop codon at a nucleotide position 526 (W178*), oligonucleotide MH408 was introduced into pGWS1384, generating pGWS1445. Furthermore, to inactivate *sclR* (SLIV_RS16665) by creating a stop codon at a nucleotide position 61 (W21*), oligonucleotide MH409 was introduced into pGWS1384, generating pGWS1446.

Following conjugation, individual exconjugants were randomly picked and streaked on SFM agar plates supplemented with 50 μg·mL^{-1} apramycin. Colonies were then streaked again on SFM plates without antibiotics, after which single colonies were selected. Genomic DNA was then extracted, and the coding sequence of *cdtR*, *cdtA* or *sclR* was PCR-amplified using primers MH410/MH411, MH412/MH413 and MH414/MH415, respectively. The PCR products were sequenced to confirm the mutations. The spacers used to create the mutations were generated using CRISPY-web[326], and are listed in Supplementary Table S3.

Construct for deletion of the jadomycin BGC

The strategy for creating deletion mutants is based on the unstable multicopy vector pWHM3[269], as described previously[271]. In this approach, we used the derivative pWHM3-oriTthat harbours *oriT*

to allow for its conjugative transfer[280]. Briefly, a knock-out construct was generated containing an apramycin resistance cassette that is flanked by the upstream and downstream regions of the targeted genes. The about 1.5 kb flanking regions of the jadomycin BGC (upstream of *jadR3* and downstream of *jadR**[300]) were amplified from *S. venezuelae* ATCC 10712 genomic DNA using primers MH416/MH417 and MH418/MH419. The apramycin resistance gene *aacC4* flanked by two *loxP* recognition sites was amplified using primers MH420/MH421. The three DNA fragments were subsequently cloned into EcoRI/HindIII-linearised pWHM3-oriT using Gibson assembly[277]. The resulting knock-out construct was designated as pGWS1447. Subsequently, the construct was introduced into *Streptomyces venezuelae* ATCC 10712 via conjugation. The desired double-crossover mutant was selected by resistance against apramycin (50 $\mu g \cdot mL^{-1}$) and sensitivity to thiostrepton (20 $\mu g \cdot mL^{-1}$). The successful replacement of the jadomycin BGC by the apramycin resistance cassette was confirmed by Sanger sequencing of the PCR product of primers MH422/MH423.

Microbial inhibition assays

To investigate the resistance to Doxo and DMdoxo in nature, we assessed our laboratory collection of actinomycetes (see section on bacterial strains above). For screening purposes, 2 µL of highly concentrated spore or mycelial stock was spotted onto SFM agar plates supplemented with increasing Doxo (Accord Healthcare Limited, UK) or DMdoxo[16] concentrations. For individual testing of *S. lividans* strains, 5 µL of spore or mycelial stock was spotted at a concentration of $1.0 \cdot 10^4$ colony forming units (CFU) per spot. After 3 to 6 days of incubation at 30 °C, growth was examined visually. Additionally, the assay was conducted using rifampicin (Boehringer Ingelheim, Germany), tetracycline hydrochloride (Duchefa Biochemie BV, Netherlands), and thiostrepton.

Adaptive laboratory evolution

For evolution experiments, strains were inoculated in 20 mL of TSB medium supplemented with a sub-inhibitory concentration of DMdoxo[16]. Once the culture reached stationary growth, an aliquot was streaked on SFM agar plates supplemented with increasing DMdoxo concentrations. Biomass from the highest concentration that supported growth was subsequently inoculated in fresh medium with the corresponding DMdoxo concentration. The process was repeated until the strain sustained growth in TSB medium supplemented with 175 µM DMdoxo. Spore or mycelial stocks were prepared from single colony isolates and the evolved strains were designated by "-Evo" (Supplementary Table S1).

MTP cultivation

Microtiter plate (MTP) cultivation was performed in a 48-well FlowerPlate (MTP-48-BOH2, Beckman Coulter, Brea, CA, USA) covered by a gas-permeable sealing foil for reduced evaporation (F-GPR-10, Beckman Coulter) in an automated cultivation device (BioLector II, Beckman Coulter). For MTP cultivation, 1 mL of TSB medium supplemented with increasing DMdoxo concentrations was inoculated with $1.0 \cdot 10^6$ $CFU \cdot mL^{-1}$ pregerminated spores. Spore stocks were pregerminated in 2xYT medium[1] for 5 hours. The shaking frequency was set to 1200 rpm, temperature was

controlled at 30 °C, and relative humidity was controlled at 85%. Back-scattered light (gain 6), pH and DO were recorded at a 15-min interval. All experiments were performed at least in triplicate.

Whole genome extraction and sequencing

Genomic DNA was extracted using phenol-chloroform extraction as described previously[1]. Sequencing was outsourced to Novogene (Cambridge, UK). PCR-free library preparation was performed to avoid sequencing biases. Sequencing was performed on an Illumina NovaSeq 6000 in paired-end mode with a read length of 150 bp.

Genome annotation of *Streptomyces* sp. Els4 and *Streptomyces* sp. Hm84 was performed using Prokka v.1.14.6[327]. AntiSMASH 7.0[297] was used under the default settings to predict BGCs in the genomic sequences of Els4, Hm84 and MBT74, which were annotated using the MiBIG database[298]. Genomic variant detection of evolved isolates of *S. lividans* TK24 and *S. peucetius* was performed using *breseq* v.0.38.1[301]. The genomes of *S. lividans* TK24 (accession NZ_CP009124.1) and *S. peucetius* var. *caesius* ATCC 27952 (accession NZ_CP022438.1) were downloaded from the NCBI database and used as reference.

RNA extraction and sequencing

TK24 and TK24-EvoA1 were streaked on minimal medium[1] agar plates supplemented with 0.5% mannitol and 1% glycerol (w/v) covered with cellophane disks at 30 °C for 24 h or 64 h. Biomass was harvested and RNA was isolated as described previously using Kirby mix[1]. RNA sequencing was outsourced to Novogene (Cambridge, UK). Ribosomal RNA was first removed from the samples and cDNA was synthesised from the purified RNA samples. Sequencing of the cDNA was performed on an Illumina NovaSeq 6000 in paired-end mode with a read length of 150 bp. Clean reads were mapped to the *S. lividans* TK24 reference sequence (accession NZ_CP009124.1). DESeq2 v.1.34.0[303] was used for differential expression analysis.

Phylogenetic analysis

The reference genomes of 625 members of the family Streptomycetaceae were downloaded from NCBI RefSeq (downloaded April 21st, 2023). The genomes of *Streptomyces coelicolor* M145 (accession GCA_000203835), *S. lividans* TK24 (accession GCF_000739105), *S. peucetius* var. *caesius* ATCC 27952 (accession GCF_002777535) and *S. venezuelae* ATCC 10712 (accession GCF_008639165) were added to the set, creating a total of 629 genomes.

To create a new anthracycline detection rule, we focused our search on four individual marker genes from *S. peucetius* (i.e. *dpsA*, *dpsB*, *dnrS* and *dnrQ*). Both *dpsA* and *dpsB* are captured by antiSMASH's[297] existing type II polyketide synthase (T2PKS) rule. To determine homologs of DnrS and DnrQ, percentage amino acid identity cutoffs were predetermined based on individual BLASTp searches against a library of experimentally verified anthracycline BGCs[266]. For profile hidden Markov model (pHMM) construction, we included homologs that shared at least 80% sequence coverage and met the resulting amino acid identity cutoffs of 47% (DnrS) and 36%

(DnrQ). The retrieved amino acid sequences were aligned with MUSCLE v.3.8.1551[328] and profiles were built using the hmmbuild tool from the HMMER v.3.3.2 suite[329] (http://hmmer.org/). A positive hit was determined when the criteria of antiSMASH's T2PKS rule was met, combined with either a DnrS or a DnrQ homolog encoding gene. Known anthracycline cluster homologs were manually searched using the hmmsearch tool from the HMMR v.3.3.2 suite to determine a bit score cutoff for true and false positive hit delineation. Using the same methodology, a detection rule was determined for the presence of homologs of *cdtAB* or *sclAB* using 100 proteins homologous to SCO3417–3418 (orthologs of CdtAB) and SCO4359–4360 (orthologs of SclAB) of *S. coelicolor*.

A maximum likelihood phylogenetic tree was constructed based on the 629 genome sequences. Eight reference genomes of Oerskovia species were used as outgroup (downloaded from NCBI RefSeq). The phylogenetic tree was generated with PhyloPhlAn v3.0[330], using DIAMOND[331] as mapping tool, MAFFT[332] for the multiple sequence alignment, trimAl[333] for alignment trimming, and RAxML[334] for generating a phylogenetic tree. iTOL[335] was used for visualisation.

Table S1. Strains used in this study.

Strain	Description	References
Escherichia coli JM109	For routine plasmid maintenance and cloning	[281]
Escherichia coli ET12567/pUZ8002	Methylation-deficient strain for conjugating plasmids into *Streptomyces*	[282]
Streptomyces coelicolor A3(2)	Wild-type strain	[1]
Streptomyces coelicolor M145	*S. coelicolor* A3(2) SCP1$^-$ SCP2$^-$	[1]
Streptomyces lividans 1326	Wild-type strain, also known as *S. lividans* 66	[1]
Streptomyces lividans TK24	*S. lividans* 1326 SLP2$^-$ SLP3$^-$	[1]
Streptomyces venezuelae ATCC 10712	Wild-type strain, producer of jadomycin	ATCC
Streptomyces galilaeus ATCC 31615	Wild-type strain, producer of aclacinomycins	ATCC
Streptomyces rimosus ATCC 10970	Wild-type strain, producer of tetracyclines	ATCC
Streptomyces peucetius var. *caesius* ATCC 27952	Wild-type strain, producer of daunorubicin and doxorubicin	[8]
Streptomyces showdoensis ATCC 15227	Wild-type strain	ATCC
Streptomyces curacoi DSM 40107	Wild-type strain	ATCC
Streptomyces sp. Els4	*Streptomyces* isolated from soil sample from Elswout, The Netherlands	Laboratory collection
Streptomyces sp. Els22	*Streptomyces* isolated from soil sample from Elswout, The Netherlands	Laboratory collection
Streptomyces sp. Els46	*Streptomyces* isolated from soil sample from Elswout, The Netherlands	Laboratory collection
Streptomyces sp. Hm84	*Streptomyces* isolated from soil sample from Himalayas, Nepal	[294]
Streptomyces sp. QL25	*Streptomyces* isolated from soil sample from Qinling Mountains, China	[294]
Streptomyces sp. MBT74	*Streptomyces* isolated from soil sample from Qinling Mountains, China	[294]
S. coelicolor-Evo	Evolved from *S. coelicolor* A3(2)*	This work
S. galilaeus-Evo	Evolved from *S. galilaeus**	This work

[continued on next page]

Table S1. *[continued]*

Strain	Description	References
S. showdoensis-Evo	Evolved from *S. showdoensis**	This work
S. curacoi-Evo	Evolved from *S. curacoi**	This work
S. peucetius-Evo	Evolved from *S. peucetius**	This work
TK24-EvoA1	Evolved from TK24*	This work
TK24-EvoB1	Evolved from TK24*	This work
TK24-EvoB2	Evolved from TK24*	This work
TK24-EvoB3	Evolved from TK24*	This work
TK24-EvoB4	Evolved from TK24*	This work
MAG401	TK24 pGWS1441 (*cdtAB*)	This work
MAG402	TK24 pGWS1442 (*sclAB*)	This work
MAG403	TK24 pGWS1443 (*drrAB*)	This work
MAG404	TK24 Δ*cdtR*	This work
MAG405	TK24 Δ*sclR*	This work
MAG406	TK24 Δ*cdtR* Δ*sclR*	This work
MAG407	TK24 Δ*cdtA*	This work
MAG408	TK24-EvoA1 Δ*cdtA*	This work
GAD05	*S. lividans* 1326 Δ*matAB*	[306]
MAG409	*S. venezuelae* ΔjadomycinBGC	This work

* Isolated from evolution experiment with DMdoxo.

Table S2. Plasmids used in this study.

Plasmid	Description	References
pSET152	*E. coli*/*Streptomyces* shuttle vector, harbouring *attP* site and integrase for phage φC31 for stable integration into the chromosomal *attB* site of *Streptomyces*, Apra^R	[274]
pWHM3-oriT	*E. coli*/*Streptomyces* shuttle vector, high copy number in *E. coli*, harbouring *oriT* site for conjugative transfer in the NdeI site, Amp^R, Thio^R	[280]
pCRISPR-cBEST	Empty vector for cytidine deaminase based base editing, Apra^R, Thio^R	[304]
pGWS1370	pSET152-derivative harbouring *tipA* promoter, Apra^R	[325]
pGWS1384	pCRISPR-cBEST-derivative with *gapdh* promoter instead of *tipA* promoter, Apra^R, Thio^R	This work
pGWS1441	pSET152-derivative with *S. lividans cdtA* and *cdtB* under control of the *ermE** promoter, Apra^R	This work
pGWS1442	pSET152-derivative with *S. lividans sclA* and *sclB* under control of the *ermE** promoter, Apra^R	This work
pGWS1443	pSET152-derivative with *S. peucetius drrA* and *drrB* under control of the *ermE** promoter, Apra^R	This work
pGWS1444	pGWS1384-derivative with a spacer targeting *cdtR* Q49, Apra^R, Thio^R	This work
pGWS1445	pGWS1384-derivative with a spacer targeting *cdtA* W178, Apra^R, Thio^R	This work
pGWS1446	pGWS1384-derivative with a spacer targeting *sclR* W21, Apra^R, Thio^R	This work
pGWS1447	pWHM3-oriT-derivative with the flanking regions of the *S. venezuelae* jadomycin BGC interspersed with the Apra^R-*loxP* cassette, Amp^R, Thio^R, Apra^R	This work

Table S3. Oligonucleotides used in this study.

Primer	Sequence (5' to 3')*
MH401	GATCGAATTCCATATGACAGTGGCCGACGCGGCG
MH402	GATCAAGCTTTCTAGAGCAGAGGTGCCCGTCCCTCG
MH403	CCACTCCACAGGAGGACCCATATGAGCGAGCGACACGCGGT
MH404	GCTTGGGCTGCAGGTCGACTCTAGAGTGGAGATCCACCGCTCCCC
MH405	GATCGAATTCCATATGAACACGCAGCCGACACG
MH406	GATCAAGCTTTCTAGACTCACACCCCCTCAACGACG
MH407	CGGTTGGTAGGATCGACGGCCGCCAGCACGGGCGGGCCCAGTTTTAGAGCTAGAAATAGC
MH408	CGGTTGGTAGGATCGACGGCCCGAGTCCCACACCTCGGCGGTTTTAGAGCTAGAAATAGC
MH409	CGGTTGGTAGGATCGACGGCGGTGTCCCACAACAGTTCGAGTTTTAGAGCTAGAAATAGC
MH410	ATGTCAGCGATCCGTCTCCT
MH411	CCGAGTGGACCCAGTAGTTC
MH412	CCGGCAGAACCTGGAGATGT
MH413	CCTTGAGTTCGTCCGCCGTG
MH414	GTCCCCCTTCCGTTCCCTTACTGA
MH415	TGGTTGACCTCCAGCAGCCAG
MH416	GTTGTAAAACGACGGCCAGTGAATTCGTGGATGTCCTCGTCGTTGA
MH417	CATCACCTCTAGACTCAGTGCCACAAGCGTCTA
MH418	CATCTCTAGATGTTCGTACTTCCTGGTGGC
MH419	AGCTATGACCATGATTACGCCAAGCTTGGTAGAAGCCCGACATACCG
MH420	TTGTGGCACTGAGTCTAGAGGTGATGGATAACTTCGTATAGCAT
MH421	AAGTACGAACATCTAGAGATGCGCGATAACTTCGT
MH422	GCCGATACAGGTCGAAGTCC
MH423	GACGCGATCTTCTCGGACC

* Restriction sites used for cloning are presented in bold face: CATATG, NdeI; TCTAGA, XbaI. Spacers used for CRISPR base editing are underlined.

Table S4. Origin and function of genes and enzymes used or discussed in this study.

Gene	Enzyme	Size (nt/aa)	Locus tag*	StrepDB SLI+	StrepDB SCO+	Catalytic function
cdtR	CdtR	642/213	SLIV_RS20695	SLI_3762	SCO3419	PadR-family transcriptional regulator
cdtA	CdtA	942/313	SLIV_RS20700	SLI_3761	SCO3418	DrrA-like ABC transporter (ATP-binding subunit)
cdtB	CdtB	783/260	SLIV_RS20705	SLI_3760	SCO3417	DrrB-like ABC transporter (permease subunit)
sclR	SclR	807/268	SLIV_RS16665	SLI_4593	SCO4358	TetR-family transcriptional regulator
sclA	SclA	1011/336	SLIV_RS16660	SLI_4594	SCO4359	DrrA-like ABC transporter (ATP-binding subunit)
sclB	SclB	843/280	SLIV_RS16655	SLI_4595	SCO4360	DrrB-like ABC transporter (permease subunit)
		705/234	SLIV_RS29140	SLI_2021	SCO1718	TetR-family transcriptional regulator
		999/332	SLIV_RS29135	SLI_2022	SCO1719	DrrA-like ABC transporter (ATP-binding subunit)
		816/271	SLIV_RS29130	SLI_2023	SCO1720	DrrB-like ABC transporter (permease subunit)
		642/213	SLIV_RS11605	SLI_5652	SCO5384	TetR-family transcriptional regulator
		783/260	SLIV_RS11610	SLI_5651	SCO5383	DrrA-like ABC transporter (ATP-binding subunit)
		750/249	SLIV_RS11615	SLI_5650	SCO5382	DrrB-like ABC transporter (permease subunit)
drrA	DrrA	993/330	CGZ69_RS24655	SLI_4076	SCO3824	ABC transporter (ATP-binding subunit)
drrB	DrrB	852/283	CGZ69_RS24650	SLI_4077	SCO3825	ABC transporter (permease subunit)

* Gene locus tags refer to the published reference genome of *S. lividans* TK24 (accession NZ_CP009124.1) and *S. peucetius* var. *caesius* ATCC 27952 (accession NZ_CP022438.1).

\+ Gene annotation in the *S. lividans* 1326 genome (SLI) and closest homologous gene in the *S. coelicolor* genome (SCO) based on the nomenclature of the StrepDB database (http://strepdb.streptomyces.org.uk).

Table S5. Genomic features of *Streptomyces* sp. Els4 and *Streptomyces* sp. Hm84.

	Els4	Hm84
Number of contigs	164	163
Largest contig	319,936	506,368
Total length	8,870,031	9,455,732
N50	125,962	118,908
CDS	7,634	8,242
rRNAs	6	6
tRNAs	89	83

Table S6. BGCs detected in the genome of *Streptomyces* sp. Els4 using antiSMASH 7.0.

Protocluster	Type	Most similar known BGC*
1	RiPP-like	-
2	T2PKS, oligosaccharide, NRPS	warkmycin (97%)
3	T1PKS, NRPS	-
4	NRPS-like, lanthipeptide-class-iv, transAT-PKS	cycloheximide (66%)
5	T1PKS	-
6	terpene, T1PKS, NRPS-like	-
7	NRPS	-
8	NRPS, NRPS-like	-
9	RiPP-like	-
10	melanin	melanin (100%)
11	T3PKS, NRPS	-
12	ectoine, butyrolactone	-
13	arylpolyene	-
14	lanthipeptide-class-iii	-
15	terpene	geosmin (100%)
16	linaridin	-
17	lanthipeptide-class-ii, lanthipeptide-class-iii	-
18	NI-siderophore	desferrioxamin B (80%)
19	terpene	-
20	NRPS	-
21	terpene	hopene (69%)
22	ectoine	ectoine (100%)
23	butyrolactone	-
24	NRPS, arylpolyene, ladderane	skyllamycin (52%)
25	T1PKS, other	-
26	NRP-metallophore, NRPS	coelichelin (90%)
27	NRPS, T1PKS	SGR PTMs (100%)
28	RiPP-like	-

[continued on next page]

Table S6. *[continued]*

Protocluster	Type	Most similar known BGC*
29	NI-siderophore	-
30	terpene	-
31	transAT-PKS, PKS-like	-
32	thiopeptide, LAP	-
33	terpene	isorenieratene (100%)
34	T3PKS	naringenin (100%)
35	NRPS	-
36	melanin	melanin (100%)
37	NRPS, NRP-metallophore	griseobactin (84%)
38	NRPS	-

* The most closely related known BGC is reported when at least 50% of the genes exhibit similarity.

Table S7. BGCs detected in the genome of *Streptomyces* sp. Hm84 using antiSMASH 7.0.

Protocluster	Type	Most similar known BGC*
1	RiPP-like	-
2	terpene	-
3	RiPP-like	-
4	siderophore	-
5	T1PKS	-
6	lanthipeptide-class-iii	-
7	NRPS, T1PKS, NRPS-like	-
8	siderophore	desferrioxamin (83%)
9	NRPS, NAPAA	-
10	siderophore	-
11	hglE-KS, T1PKS	-
12	terpene	geosmin (100%)
13	T2PKS	spore pigment (83%)
14	melanin	-
15	RRE-containing	-
16	nucleoside	-
17	LAP, thiopeptide	-
18	ectoine	ectoine (100%)
19	T3PKS	-
20	NAPAA	-
21	NRPS	-
22	terpene	albaflavenone (100%)
23	NRPS	-
24	RiPP-like	-

[continued on next page]

Table S7. *[continued]*

Protocluster	Type	Most similar known BGC*
25	terpene	carotenoid (63%)
26	T3PKS	alkylresorcinol (100%)
27	melanin	melanin (71%)
28	terpene	hopene (84%)
29	indole	-
30	T1PKS, PKS-like, NRPS-like	-
31	butyrolactone	-
32	T1PKS, ectoine	-
33	T1PKS, butyrolactone	-
34	butyrolactone	-
35	T1PKS	-
36	T1PKS	-
37	T2PKS	jadomycin (85%)

* The most closely related known BGC is reported when at least 50% of the genes exhibit similarity.

Table S8. BGCs detected in the genome of *Streptomyces* sp. MBT74 using antiSMASH 7.0.

Protocluster	Type	Most similar known BGC*
1	T2PKS	spore pigment (83%)
2	RiPP-like	-
3	phenazine	-
4	melanin	-
5	NAPAA	-
6	NI-siderophore	-
7	NRPS	-
8	terpene	albaflavenone (100%)
9	T3PKS	flaviolin (100%)
10	NRPS-like, T1PKS, NRPS	-
11	ectoine	ectoine (100%)
12	RiPP-like	-
13	terpene	geosmin (100%)
14	NI-siderophore	desferrioxamin (83%)
15	T1PKS	-
16	thiopeptide, LAP	-
17	T3PKS	alkylresorcinol (100%)
18	RiPP-like	-
19	NI-siderophore	-
20	terpene	hopene (61%)
21	butyrolactone	-

* The most closely related known BGC is reported when at least 50% of the genes exhibit similarity.

Table S9. Putative anthracycline BGCs detected in the reference genomes of 625 members of the family Streptomycetaceae.

Location	Organism*	Most similar known BGC (similarity)
NZ_AGBF01000013.1 :3475–83811	*S. zinciresistens* K42	cytorhodin (82%)
NZ_BMML01000021.1 :144082–218040	*S. fuscichromogenes* CGMCC 4.7110	aranciamycin (78%)
NZ_BMQK01000002.1 :535976–616788	*S. ruber* JCM 3131	cytorhodin (50%)
NZ_BMSO01000019.1 :12468–93240	*S. bellus* JCM 4292	cosmomycin D (60%)
NZ_BMTM01000017.1 :10575–103634	*S. janthinus* JCM 4387	cytorhodin (84%)
NZ_BMUK01000008.1 :375570–469210	*S. purpurascens* JCM 4509	cytorhodin (84%)
NZ_BMUP01000006.1 :475604–568638	*S. violarus* JCM 4534	cytorhodin (84%)
NZ_BMVC01000018.1 :18422–109983	*S. finlayi* JCM 4637	kosinostatin (77%)
NZ_BMVY01000030.1 :0–66622	*S. tauricus* JCM 4837	cinerubin B (100%)
NZ_BMWA01000001.1 :309989–403064	*S. viridiviolaceus* JCM 4855	cytorhodin (82%)
NZ_BMWD01000002.1 :353044–441234	*S. fructofermentans* JCM 4956	cinerubin B (100%)
NZ_BNBF01000007.1 :191587–279349	*S. capoamus* JCM 4253	cinerubin B (100%)
NZ_CP020700.1 :5211320–5289097	*S. tsukubensis* NRRL 18488	komodoquinone B (97%)
NZ_CP023693.1 :6171688–6259901	*S. cinereoruber* ATCC 19740	cytorhodin (82%)
NZ_CP023694.1 :7072200–7152971	*S. coeruleorubidus* ATCC 13740	cosmomycin D (62%)
NZ_CP023703.1 :6303449–6391243	*S. galilaeus* ATCC 14969	cinerubin B (100%)
NZ_CP029188.1 :6338721–6433635	*S. tirandamycinicus* HNM0039	cosmomycin C (100%)
NZ_FMZK01000002.1 :69913–150677	*S. prasinopilosus* CGMCC 4.3504	cytorhodin (47%)
NZ_JAGPYQ010000001 .1:2767761–2855941	*S.* sp. BH-SS-21	cinerubin B (100%)
NZ_JAIQLH010000037.1 :0–56893	*S. huiliensis* SCA2-4	aranciamycin (78%)

[continued on next page]

Table S9. *[continued]*

Location	Organism*	Most similar known BGC (similarity)
NZ_JAPELN010000001.1 :6826013–6913829	*S. bobili* NBC_00018	cinerubin B (100%)
NZ_JAPEPV010000002.1 :126993–202530	*S. viridodiastaticus* NBC_01548	kosinostatin (35%)
NZ_JNWJ01000033.1 :12534–95124	*S. yerevanensis* NRRL B-16943	griseorhodin A (93%)
NZ_JNZG01000006.1 :170654–255869	*S. erythrochromogenes* NRRL B-2112	komodoquinone B (100%)
NZ_JODM01000005.1 :177751–265519	*S. violaceorubidus* NRRL B-16381	cinerubin B (100%)
NZ_KQ948766.1 :0–76988	*S. griseoruber* DSM 40281	cinerubin B (100%)
NZ_KQ948995.1 :59575–152007	*S. resistomycificus* DSM 40133	steffimycin D (88%)
NZ_KZ679040.1 :471754–560086	*S. dioscori* A217	cinerubin B (100%)
NZ_LAQS01000005.1 :116538–203674	*S. showdoensis* ATCC 15227	komodoquinone B (65%)
NZ_NDXL01000001.1 :1980945–2061737	*S. kasugaensis* BCRC 12349	cytorhodin (49%)
NZ_SUMB01000006.1 :333894–423185	*S. piniterrae* jys28	griseorhodin A (87%)
NZ_VAWE01000001.1 :2640914–2721684	*S. marianii* ICN19	cosmomycin D (62%)

* *Streptomyces* abbreviated to *S.*

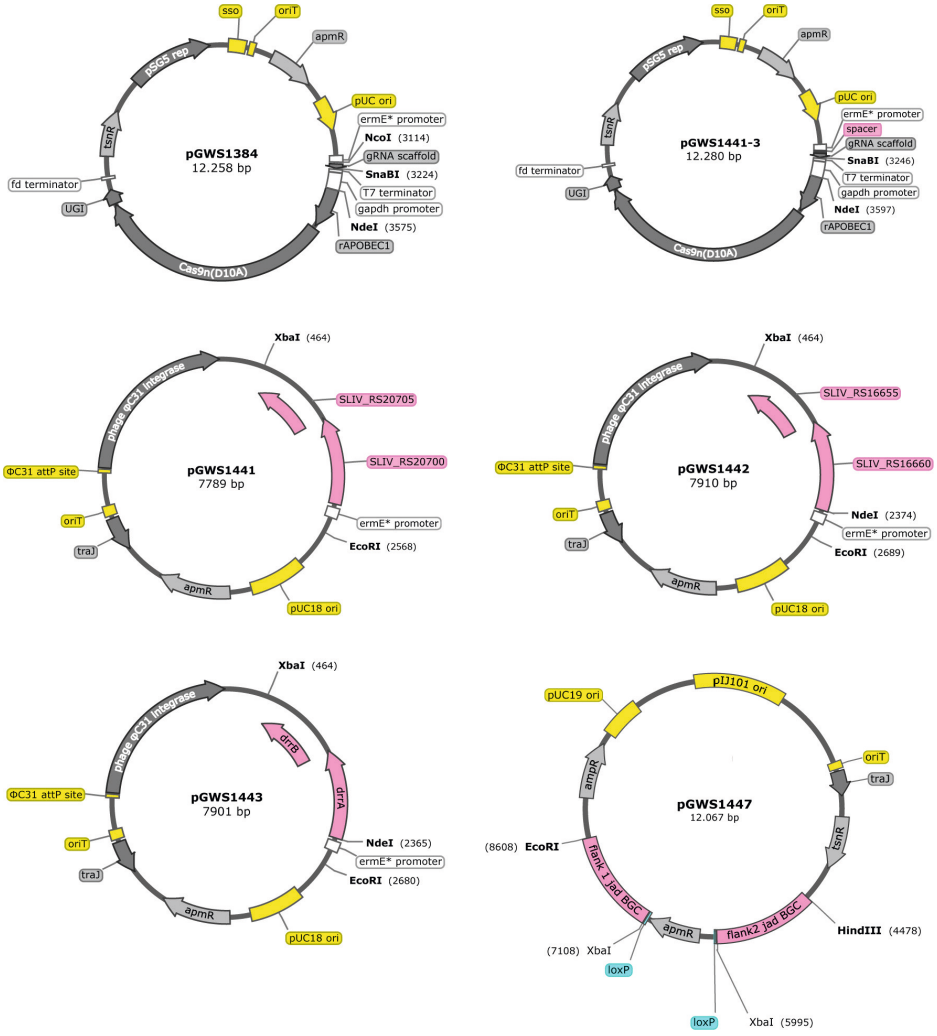

Figure S1. Plasmid maps of constructs used in this study. Restriction sites used for cloning are indicated. Resistance cassettes are abbreviated as: *ampR*, ampicillin; *apmR*, apramycin; *tsnR*, thiostrepton.

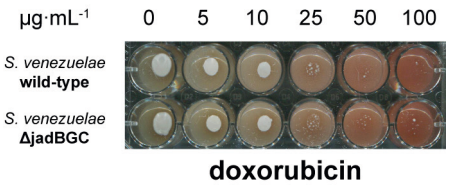

Figure S2. Impact of the jadomycin BGC deletion on doxorubicin resistance in *S. venezuelae*. Wild-type *S. venezuelae* and a mutant strain with the entire jadomycin BGC deleted (MAG409) were spotted on SFM agar plates supplemented with 5 to 100 µg·mL-1 (i.e. 9.2 to 184 µM) Doxo, and incubated at 30 °C for 3 days. Deletion of the jadomycin BCG did not affect resistance to Doxo.

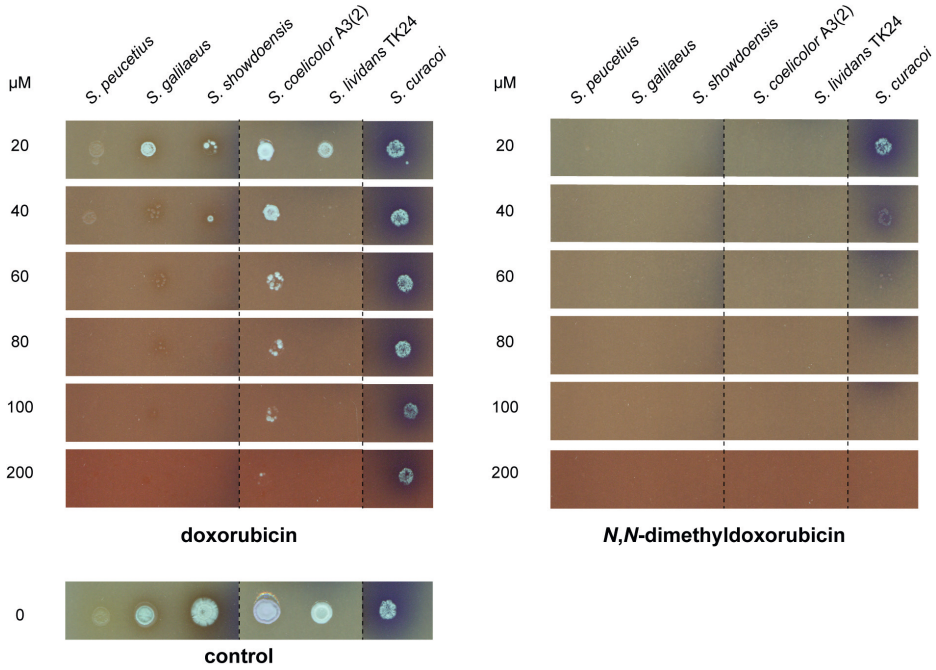

Figure S3. Evaluation of anthracycline resistance of parental strains used in evolution experiment. Parental strains of the evolution experiment were spotted at high density on SFM agar plates supplemented with 20 to 200 μM Doxo or DMdoxo, and incubated at 30 °C for 3 days.